Cell Reports

Resource

Recombinase-Dependent Mouse Lines for Chemogenetic Activation of Genetically Defined Cell Types

Graphical Abstract

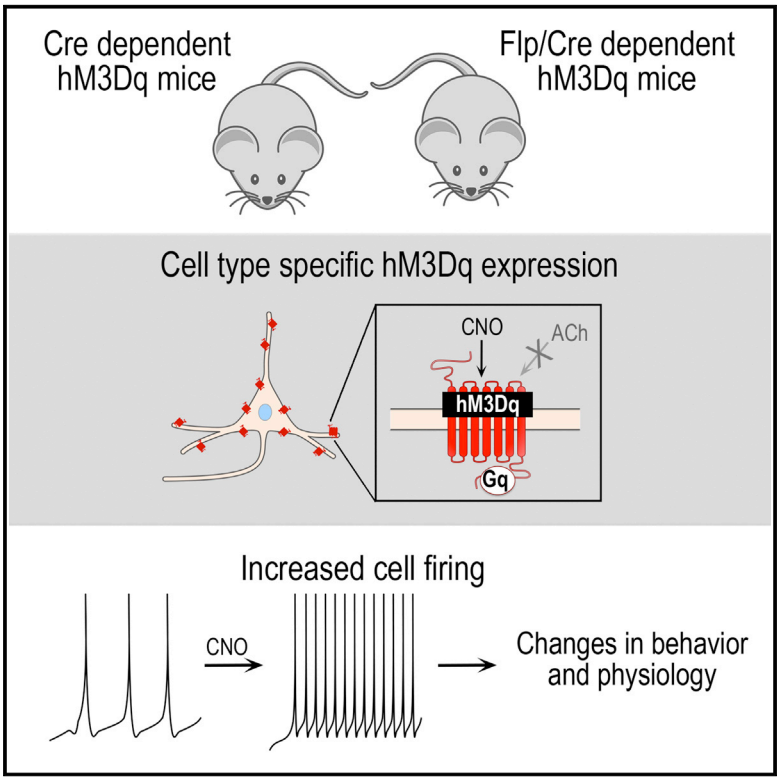

Highlights

- Recombinase-responsive mice express hM3Dq DREADD for induction of cellular activity
- Targeting of hM3Dq to cell body and dendrites increases effective expression levels
- mCherry fusion permits visualization of hM3Dq^{+} cells in vivo
- Dose-dependent activation of hM3Dq drives behavioral and physiological changes

Authors

Natale R. Sciolino, Nicholas W. Plummer, Yu-Wei Chen, ..., Serena M. Dudek, Zoe A. McElligott, Patricia Jensen

Correspondence

patricia.jensen@nih.gov

In Brief

Sciolino et al. develop Cre- and Flp/Cre-responsive mouse lines for non-invasive expression of hM3Dq in genetically defined cells. A targeted fusion protein is designed to increase effective expression level, enabling dose-dependent induction of cellular activity in diverse cell types.

Sciolino et al., 2016, Cell Reports *15*, 2563–2573
June 14, 2016 Array
http://dx.doi.org/10.1016/j.celrep.2016.05.034

Cell Reports
Resource

Recombinase-Dependent Mouse Lines for Chemogenetic Activation of Genetically Defined Cell Types

Natale R. Sciolino,[1,5] Nicholas W. Plummer,[1,5] Yu-Wei Chen,[1] Georgia M. Alexander,[1] Sabrina D. Robertson,[2] Serena M. Dudek,[1] Zoe A. McElligott,[3,4] and Patricia Jensen[1,*]
[1]Neurobiology Laboratory, Department of Health and Human Services, National Institute of Environmental Health Sciences (NIEHS), NIH, Research Triangle Park, NC 27709, USA
[2]Biotechnology Program, Department of Molecular Biomedical Sciences, North Carolina State University, Raleigh, NC 27695, USA
[3]Bowles Center for Alcohol Studies, University of North Carolina School of Medicine, Chapel Hill, NC 27514, USA
[4]Department of Psychiatry, University of North Carolina School of Medicine, Chapel Hill, NC 27514, USA
[5]Co-first author
*Correspondence: patricia.jensen@nih.gov
http://dx.doi.org/10.1016/j.celrep.2016.05.034

SUMMARY

Chemogenetic technologies, including the mutated human G_q-coupled M3 muscarinic receptor (hM3Dq), have greatly facilitated our ability to directly link changes in cellular activity to altered physiology and behavior. Here, we extend the hM3Dq toolkit with recombinase-responsive mouse lines that permit hM3Dq expression in virtually any cell type. These alleles encode a fusion protein designed to increase effective expression levels by concentrating hM3Dq to the cell body and dendrites. To illustrate their broad utility, we targeted three different genetically defined cell populations: noradrenergic neurons of the compact, bilateral locus coeruleus and two dispersed populations, *Camk2a*+ neurons and *GFAP*+ glia. In all three populations, we observed reproducible expression and confirmed that activation of hM3Dq is sufficient to dose-dependently evoke phenotypic changes, without extreme phenotypes associated with hM3Dq overexpression. These alleles offer the ability to non-invasively control activity of diverse cell types to uncover their function and dysfunction at any developmental stage.

INTRODUCTION

Since their initial description less than 10 years ago (Armbruster et al., 2007), the engineered G protein-coupled receptors known as designer receptors exclusively activated by designer drugs (DREADDs) have proven invaluable for linking cellular activity to changes in physiology and behavior. Among the most frequently used DREADDs is hM3Dq, a mutated G_q-coupled human M3 muscarinic receptor that is activated exclusively by the designer drug clozapine *N*-oxide (CNO), but not its native ligand acetylcholine. By coupling to endogenous signal transduction pathways, hM3Dq has provided insight into the unique functions of cells as diverse as neurons, glia, pancreatic β cells, and hepatocytes (as reviewed in Urban and Roth, 2015). In neurons, activation of hM3Dq by CNO leads to calcium influx and increased cell firing, thereby promoting neuronal excitability (Alexander et al., 2009). Thus, hM3Dq has been of particular value for identifying the functions encoded by specific neurons in the freely behaving animal.

Previous methods for delivery of hM3Dq to cells in vivo have included viral vectors, transgenes, and targeted knockin mouse lines (Urban and Roth, 2015; Zhu and Roth, 2014). Each of these strategies drives hM3Dq expression at levels sufficient for behavioral or physiological analyses, but each has limitations. The most commonly used method for delivery of hM3Dq is injection of viral vectors. Although these constructs often generate very high levels of hM3Dq expression, overexpression may result in extreme phenotypes of questionable physiological relevance. Furthermore, the requirement for direct injection limits the use of viruses prenatally and in juvenile/adolescent animals. Multiple injections are required to target dispersed or bilateral cell populations, increasing the possibility of experimentally significant trauma and variable expression among experimental subjects. Some of the experimental limitations of viral vectors can be overcome by the use of transgenes. Given an appropriate promoter, transgene expression can be achieved non-invasively in anatomically dispersed populations at any stage of development. However, each targeted cell population requires generation of a unique transgenic line, and multi-copy transgene arrays can result in unpredictable expression levels. In contrast, single-copy knockin alleles, particularly recombinase-responsive constructs, offer consistent, reproducible expression and the broadest range of possible cellular targets by partnership with existing cell-type-specific recombinase driver lines. However, expression levels of single-copy alleles are likely to be lower than those achieved with viruses or transgenes.

To overcome these experimental challenges, we generated two recombinase-responsive knockin alleles that complement existing hM3Dq constructs by permitting non-invasive targeting of hM3Dq to the cell body (soma) and dendrites of genetically defined cells. This somatodendritic localization is designed to

concentrate hM3Dq, thus increasing its effective expression level. Our Cre-responsive allele permits expression of hM3Dq in genetically defined cell populations by taking advantage of the many available cell-type-specific Cre driver alleles. Because control by a single recombinase defines relatively broad classes of cells, we also have generated a Flp/Cre-responsive allele that restricts hM3Dq to the narrow intersection of two broader recombinase expression domains. hM3Dq is expressed only in those cells that have expressed Flp and Cre drivers, each controlled by the promoters of different genes, thus allowing functional manipulation of cell populations that cannot be defined by a single gene.

In this paper, we confirm that both alleles permit expression of an hM3Dq-mCherry fusion protein detectable at single-cell resolution in live and fixed tissue from embryos or adult mice. Furthermore, we demonstrate the broad utility of the alleles in three different cell populations: noradrenergic neurons of the small, bilateral locus coeruleus (LC) and two dispersed cell populations, *Camk2a*+ neurons and *GFAP*+ glia. In a proof-of-principle experiment using our Flp/Cre-responsive allele, we demonstrate that CNO increases neuronal firing of hM3Dq-expressing LC neurons in vitro. We then demonstrate the in vivo effectiveness of the Flp/Cre-responsive allele by inducing anxiety-like behavior observed following activation of LC neurons (McCall et al., 2015). Next we evaluate the in vivo utility of our Cre-responsive allele by evoking physiological signatures ascribed to activation of *Camk2a*+ neurons (Alexander et al., 2009) and *GFAP*+ glia (Agulhon et al., 2013), specifically hippocampal gamma oscillations and profound depression of body temperature, respectively. Collectively, these findings demonstrate that our hM3Dq alleles permit activation of genetically defined cell populations in a reproducible, dose-dependent manner and are valuable additions to the DREADD toolkit.

RESULTS

Generation of Flp/Cre and Cre Recombinase-Responsive Alleles for Somatodendritic Targeting of hM3Dq

To ensure expression of our Flp/Cre-responsive (Rosa-CAG-FRT-lox-hM3Dq [*RC*::*FL-hM3Dq*]) and Cre-responsive (Rosa-CAG-lox-hM3Dq [*RC*::*L-hM3Dq*]) alleles in a wide range of cell types and developmental stages, we used a synthetic CAG promoter (Niwa et al., 1991) and targeted the *Gt*(*ROSA*)*26Sor* locus (Friedrich and Soriano, 1991) in mouse embryonic stem cells (Figure 1A). In *RC*::*FL-hM3Dq*, an FRT-flanked transcriptional stop cassette (Sauer, 1993) following the CAG promoter prevents transcription of all downstream sequence until it is excised by Flp recombinase. The allele also encodes EGFP and an hM3Dq-mCherry fusion protein with a C-terminal epitope (2ACT88) that mediates localization of the hM3Dq receptor to the cell body (soma) and dendrites (Xia et al., 2003). To prevent expression in the absence of Cre recombination, the hM3Dq-mCherry cDNA is inverted in a Cre-dependent FLEx switch consisting of two pairs of antiparallel lox sites (Atasoy et al., 2008; Schnütgen et al., 2003). Cre activity results in inversion of hM3Dq-mCherry to the proper orientation for transcription. *RC*::*FL-hM3Dq* expresses EGFP following Flp-mediated recombination and hM3Dq-mCherry after recombination by both Flp and Cre. *RC*::*L-hM3Dq* lacks the FRT-flanked stop cassette but is otherwise identical to *RC*::*FL-hM3Dq*. Therefore, *RC*::*L-hM3Dq* expresses EGFP in the absence of recombinase activity and hM3Dq-mCherry after Cre-mediated recombination. Because the recombination events are irreversible, cells express hM3Dq-mCherry continuously, even if recombinase expression is transient. Thus, *RC*::*L-hM3Dq* expresses hM3Dq-mCherry in broad populations of cells defined by a single promoter that drives Cre expression. *RC*::*FL-hM3Dq* allows restriction of hM3Dq-mCherry to more specific subpopulations defined by shared expression of Flp and Cre driven by different promoters.

To confirm that the CAG promoter is broadly active and that hM3Dq-mCherry expression is efficiently controlled by recombinase activity, we examined EGFP and mCherry fluorescence in *RC*::*FL-hM3Dq* and *RC*::*L-hM3Dq* embryos and adults. In the absence of recombinase activity, we observed neither EGFP nor mCherry expression in *RC*::*FL-hM3Dq* embryos (Figure 1B) and adult brain (Figure S1) due to the intact stop cassette and FLEx switch. Following germline excision of the FRT-flanked stop cassette (*RC*::*L-hM3Dq)*, we observed ubiquitous expression of EGFP, but no mCherry. Subsequent germline recombination of the FLEx switch in *RC*::*L-hM3Dq* mice resulted in ubiquitous mCherry expression in both embryos and adult brain (Figures 1B and S1). Thus, the CAG promoter is active throughout development, and both the FRT-flanked stop cassette and Cre-dependent FLEx switch are capable of controlling expression of the proteins encoded by our two alleles.

To demonstrate the widest possible expression of hM3Dq-mCherry, we crossed *RC*::*FL-hM3Dq* to the ubiquitously expressed *ACTB-Flpe* (Rodríguez et al., 2000) and *ACTB-cre* (Lewandoski et al., 1997) recombinase drivers. We observed hM3Dq-mCherry expression in a wide variety of cell types throughout the brain (Figure 2). Next we used cell-type-specific drivers to test whether our alleles can direct somatodendritic localization of hM3Dq-mCherry in restricted cell populations. We used *RC*::*L-hM3Dq* in combination with *Camk2a-cre* (Tsien et al., 1996) or *GFAP-creERT2* (Casper et al., 2007) transgenes for expression of hM3Dq-mCherry in neurons or glia, respectively. As expected, mCherry fluorescence was restricted to the soma and dendrites of neurons in the well-documented expression domain of the *Camk2a-cre*-transgene (Sonner et al., 2005), including cortical and hippocampal neurons (Figures 3A, 3B, and S2). Using the glial-specific *GFAP-creERT2* transgene, we observed restricted mCherry fluorescence in the soma and processes of glia defined by *Gfap* expression (Figures 3C and S3). To demonstrate intersectional Flp/Cre control of *RC*::*FL-hM3Dq*, we targeted a population of noradrenergic neurons defined by a shared history of both $En1^{cre}$ and Dbh^{Flpo} expression (Robertson et al., 2013). This combination of recombinase drivers restricts hM3Dq-mCherry expression to a subpopulation of noradrenergic neurons (hereafter designated LC complex), which encompasses 99.8% of the compact LC and a portion of the dorsal subcoeruleus and A7 noradrenergic nuclei (Robertson et al., 2013; Plummer et al., 2015). As expected, mCherry fluorescence was restricted to the soma and dendrites of the LC complex (Figures 3D and S4). All remaining noradrenergic neurons, expressing only Dbh^{Flpo}, were labeled with EGFP (Figure S4).

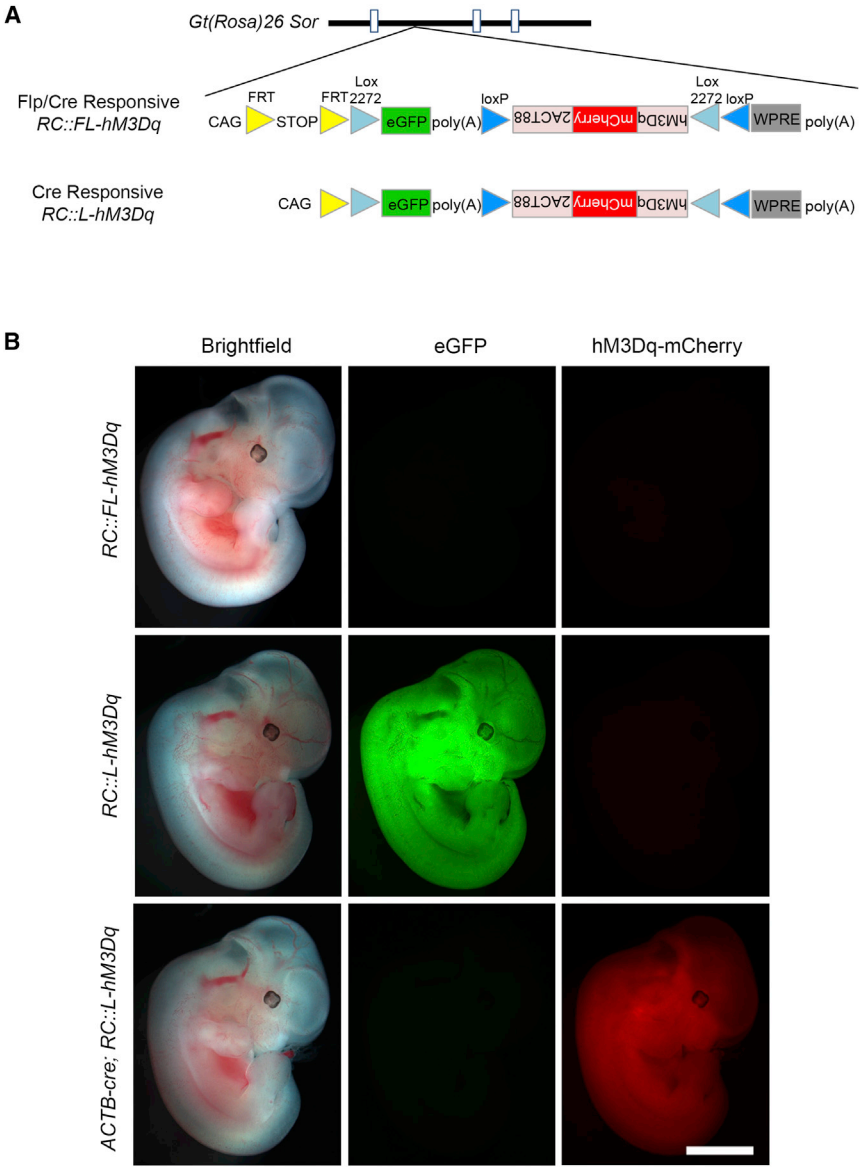

Figure 1. Recombinase-Responsive Alleles for Somatodendritic Targeting of hM3Dq

(A) Schematic diagrams of *RC*::*FL-hM3Dq* (Jackson Lab JAX#026942) and *RC*::*L-hM3Dq* (Jackson Lab JAX#026943) shown in relation to the *Gt(ROSA)26Sor* locus. In both alleles, a CAG promoter drives gene expression. *RC*::*FL-hM3Dq* expresses EGFP after Flp-mediated excision of the FRT-flanked His3-SV40 stop cassette (STOP). hM3Dq-mCherry fusion protein is expressed after excision of the stop cassette and recombination of lox2272 and loxP sites constituting the Cre-dependent FLEx switch. *RC*::*L-hM3Dq* expresses EGFP ubiquitously and hM3Dq-mCherry after Cre-mediated recombination of the FLEx switch. 2ACT88, C-terminal fragment of HTR2A; WPRE, woodchuck hepatitis virus posttranscriptional regulatory element; poly(A), bovine growth hormone polyadenylation signal.

(B) Native EGFP and mCherry fluorescence in E11.5 embryos. Top: absence of fluorescence in *RC*::*FL-hM3Dq* heterozygote confirms that the FRT-flanked stop cassette blocks expression in the absence of Flp activity. Middle: ubiquitous EGFP fluorescence, but no mCherry, in *RC*::*L-hM3Dq* heterozygote confirms that the FLEx switch blocks hM3Dq expression in the absence of Cre activity. Bottom: ubiquitous mCherry fluorescence observed after crossing *RC*::*L-hM3Dq* with a ubiquitously expressed *ACTB-cre* transgene (Lewandoski et al., 1997) confirms recombination of the Cre-dependent FLEx switch. Scale bar, 2 mm.

Unexpectedly, we observed faint mCherry fluorescence in cerebellar Purkinje cells that have expressed *En1*^{cre}, but not *Dbh*^{Flpo} (Figure S5A). The absence of ectopic EGFP expression suggested that the ectopic mCherry results from mRNA splicing that occurs after Cre-mediated recombination of the FLEx switch, rather than failure of the FRT-flanked stop cassette. To test this hypothesis, we performed RT-PCR analysis of cerebellum RNA and identified mRNA from *RC*::*FL-hM3Dq* in cells that had recombined the FLEx switch (Figure S5B). Due to a cryptic splice acceptor within the hM3Dq cDNA, this mRNA encoded mCherry, but not the full hM3Dq-mCherry fusion. These experiments confirm that our alleles faithfully express hM3Dq-mCherry in the defined recombinase expression domains, demonstrating they can deliver hM3Dq to a variety of cell types limited only by the availability of Flp and Cre driver lines.

Selective hM3Dq-Mediated Activation of Noradrenergic Neurons In Vitro

To evaluate whether the level of hM3Dq expressed from *RC*::*FL-hM3Dq* is sufficient to alter cellular activity, we carried out whole-cell patch-clamp recordings of noradrenergic neurons in the LC complex that express either hM3Dq-mCherry (*En1*^{cre}; *Dbh*^{Flpo}; *RC*::*FL-hM3Dq* triple heterozygotes) or EGFP (*Dbh*^{Flpo}; *RC*::*FL-hM3Dq* controls) (Figure 4A). Fluorescence in the LC complex was readily detected in acute slice preparations (Figure 4B). To evaluate whether CNO would depolarize hM3Dq-expressing neurons, we recorded in the presence of the Na^+ channel blocker TTX (500 nM) or TTX plus the L-type Ca^{2+} channel blocker nimodipine (1 μm) to eliminate network effects and oscillations. Average resting membrane potential was −56.0 ± 11.0 mV, consistent with prior observations of LC neurons (Williams et al., 1984; de Oliveira et al., 2010). Bath application of 10 μM CNO depolarized hM3Dq-mCherry+ LC complex neurons recorded in TTX (4.04 ± 0.91 mV, n = 5 neurons) or TTX + nimodipine (1.60 ± 0.27 mV, n = 4 neurons). The depolarization measured under the two recording conditions was not statistically different (p = 0.20), and therefore data were combined, yielding an average depolarization of 2.95 ± 0.48 mV (Figure 4C). In

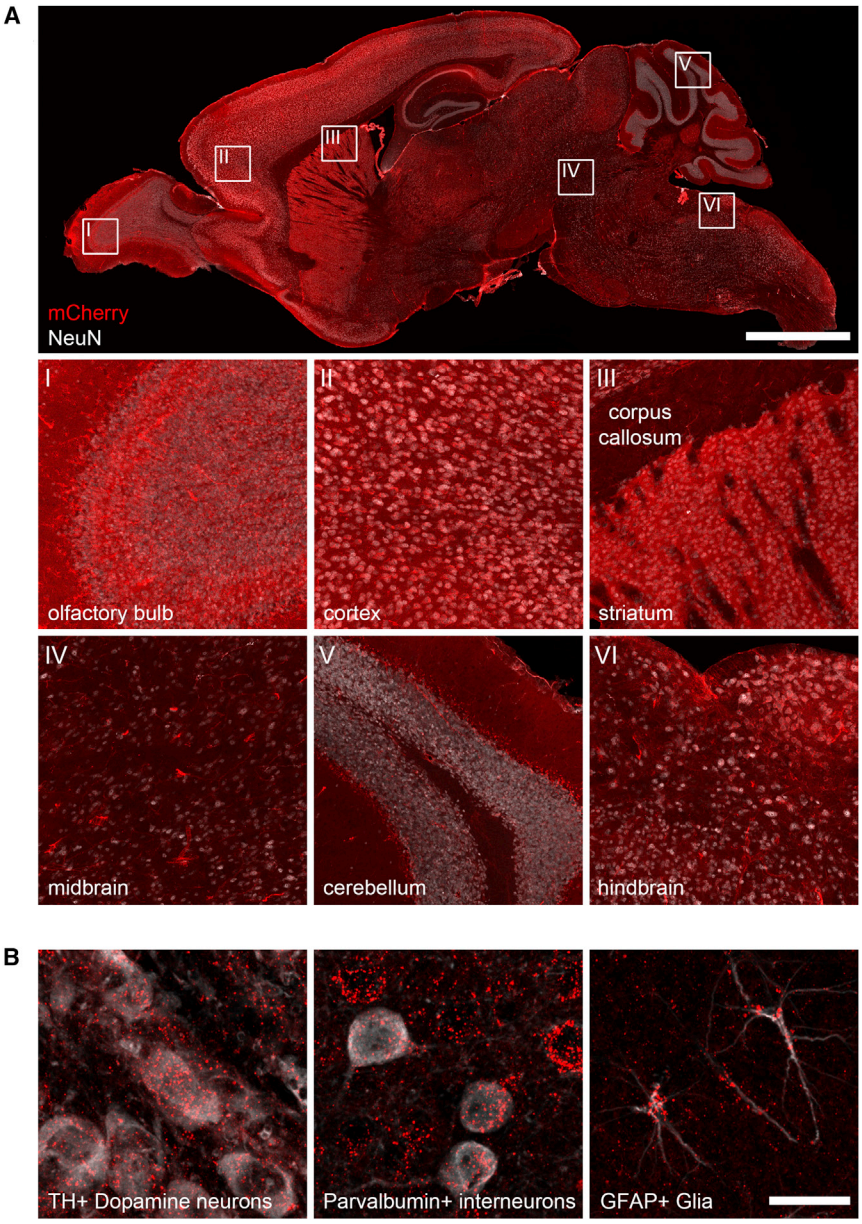

Figure 2. Widespread Expression of hM3Dq-mCherry after Recombination of *RC::FL-hM3Dq* by Ubiquitous Flp and Cre Driver Alleles

(A) Sagittal section of *ACTB-cre*; *ACTB-Flpe*; *RC::FL-hM3Dq* brain immunolabeled for mCherry (red) and the neuronal marker NeuN (white). Boxes show location of magnified images (below). Following ubiquitous recombinase expression, mCherry is observed throughout the brain. Fluorescence is attenuated in regions with a high proportion of axons (e.g., corpus callosum), consistent with somatodendritic targeting of hM3Dq-mCherry. Scale bars, 2,000 μm (full sagittal section) and 244 μm (magnified images).

(B) Sections of *ACTB-cre*; *ACTB-Flpe*; *RC::FL-hM3Dq* brain immunolabeled for mCherry (red) and markers of neuronal and glial subtypes (white). hM3Dq-mcherry is observed in midbrain dopaminergic neurons labeled for tyrosine hydroxylase (TH), cortical interneurons labeled for parvalbumin, and astrocytes labeled for glial fibrillary acidic protein (GFAP). Scale bar, 20 μm.

contrast, CNO had no effect on membrane potential of EGFP+ control neurons (Figures 4B and 4C). Depolarization by 50 μM NMDA, however, confirmed that these cells were healthy and responsive (Figure 4B). In the absence of CNO, hM3Dq-mCherry+ and EGFP+ neurons exhibited similar baseline membrane potential, capacitance, and membrane and input resistance (Figure 4C; data not shown), suggesting that *mere* expression of hM3Dq-mCherry does not impact membrane properties.

To test whether expression of hM3Dq is sufficient to evoke neuronal firing, we next performed cell-attached recordings in the absence of TTX and nimodipine. Bath application of CNO (10 μM) increased the firing rate of hM3Dq-mCherry+ LC neurons by an average of 75.6% ± 30.0% above baseline activity (0.91 ± 0.08 Hz; n = 6 cells; $p < 0.001$; Figures 4D and 4E). To confirm that the ectopically labeled Purkinje cells do not express functional hM3Dq-mCherry fusion protein, we also performed whole-cell recordings of these cells. Consistent with our identification of a nonfunctional mRNA, membrane potential of mCherry+ Purkinje cells was not altered by 10 μM CNO (Figure S5C). Taken together, these results demonstrate that the level of hM3Dq-mCherry expressed from *RC::FL-hM3Dq* permits chemogenetic activation of an intersectional subpopulation defined by expression of Cre and Flp.

In Vivo Activation of the LC Complex Induces Anxiety-like Behavior and Suppresses Locomotion

We assessed the in vivo utility of our dual recombinase-responsive allele by testing whether expression of hM3Dq can alter anxiety-like behavior. Optogenetic stimulation of LC neurons at high, tonic frequency (5 Hz) prior to testing evokes anxiety-like behavior and suppresses locomotion (McCall et al., 2015). To test whether hM3Dq would evoke similar responses, we treated mice with CNO (1 or 5 mg/kg, intraperitoneally [i.p.]) or vehicle before testing in the following three assays: the elevated plus maze (EPM), light-dark box (LDB), and open-field test (OFT). In all three assays, CNO dose-dependently evoked anxiety-like responses and concomitantly suppressed locomotion of mice expressing hM3Dq-mCherry in the LC complex (Figure 5; Table S1). CNO at 5 mg/kg significantly induced anxiety-like behavior by reducing exploration within the aversive areas of the tests, including open arms of the EPM (Figure 5A), light compartment

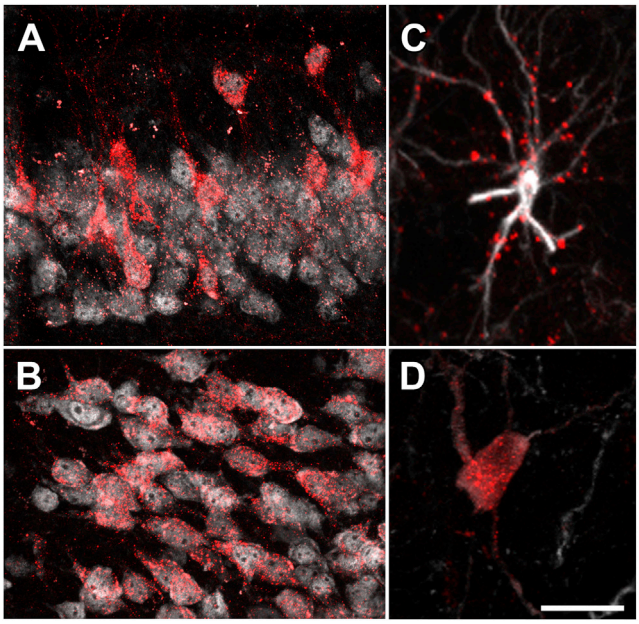

Figure 3. Somatodendritic Targeting of hM3Dq-mCherry in Neurons and Glia

(A) Hippocampal CA3 neurons in a *Camk2a-cre*; *RC*::*L-hM3Dq* brain immunolabeled for mCherry (red) and nuclear NeuN (white) are shown.

(B) Cortical neurons from a *Camk2a-cre*; *RC*::*L-hM3Dq* brain immunolabeled for mCherry (red) and NeuN (white) are shown.

(C) Cortical astrocyte from a *GFAP-CreERT2*; *RC*::*L-hM3Dq* brain immunolabeled for mCherry (red) and GFAP (white) is shown.

(D) Noradrenergic neuron from an $En1^{Cre}$; Dbh^{Flpo}; *RC*::*FL-hM3Dq* brain immunolabeled for mCherry (red) and tyrosine hydroxylase (white). Images are taken from coronal sections. Scale bars, 40 (A and B) and 20 μm (C and D).

of the LDB (Figure 5B), and center zone of the OFT (Figures 5C and S6) compared to vehicle. Both doses of CNO also suppressed locomotion, as shown by reduced closed-arm entries in the EPM and distance ambulated in LDB and OFT compared to vehicle (Figure 5). CNO had no effect on behavioral performance of all littermate controls (Figure S7). In addition, mice expressing hM3Dq and all littermate controls were indistinguishable when treated with vehicle (Figure S7). Collectively, these data demonstrate that *RC*::*FL-hM3Dq* faithfully expresses hM3Dq at levels that permit sensitive control of an intersectionally targeted neuronal subpopulation and recapitulates behavioral phenotypes evoked by optogenetic stimulation.

Dose-Dependent Activation of hM3Dq Drives Gamma Oscillations in Hippocampal Neurons In Vivo

Next we assessed the efficacy of our single recombinase-responsive allele by testing whether hM3Dq can activate a dispersed neuronal population. In the original description of a tetracycline-controlled hM3Dq transgene, hippocampal gamma power was progressively evoked in *Camk2a*+ neurons following escalating doses of CNO (Alexander et al., 2009). To determine whether our Cre-responsive allele would evoke similar neural activity, we used the *Camk2a-cre* transgene (Tsien et al., 1996) to drive hM3Dq-mCherry expression (Figure 6A). We recorded local field potentials in CA3 of the hippocampus of mice expressing hM3Dq-mCherry in *Camk2a*+ neurons (*Camk2a-cre*; *RC*::*L-hM3Dq*) and littermate controls. Consistent with the original study, we found that CNO dose-dependently increased hippocampal gamma power (50–80 Hz) in mice expressing hM3Dq-mCherry (Figures 6B and 6C). Doses of CNO as low as 1 mg/kg increased peak gamma power compared to vehicle. The 10-mg/kg dose significantly increased gamma power 20 min following CNO injection, and gamma returned to baseline levels an hour thereafter (Figure 6C). In all littermate controls, CNO had no effect on peak gamma power (Figure 6C). These results confirm that *RC*::*L-hM3Dq* can be used to efficiently and precisely control the activity of neuronal populations at levels measurable by in vivo electrophysiology.

In Vivo Activation of hM3Dq Expressed in Glia Elicits Hypothermia

We further assessed the broad utility of *RC*::*L-hM3Dq* by targeting a dispersed population of non-neuronal cells. Activation of hM3Dq expressed in glia by a *GFAP-hM3Dq* transgene previously has been shown to induce hypothermia (Agulhon et al., 2013). To determine whether *RC*::*L-hM3Dq* can recapitulate this effect, we used the tamoxifen-inducible *GFAP-creERT2* transgene (Casper et al., 2007) to drive hM3Dq-mCherry expression in glia (Figure 7A). Hypothermia was observed in mice expressing hM3Dq-mCherry in *Gfap*+ glia starting at 40 min after injection of CNO (5 mg/kg) and persisted until the test was stopped at 90 min due to dangerously low body temperature (Figure 7B). In contrast, CNO did not alter body temperature in littermate controls (Figure 7C). Furthermore, we observed no effect of vehicle on body temperature (Figures 7B and 7C). Collectively, these data demonstrate that *RC*::*L-hM3Dq* permits activation of dispersed non-neuronal populations at levels sufficient to evoke lasting physiological changes.

DISCUSSION

The experiments described here demonstrate that our Flp/Cre- and Cre-responsive hM3Dq alleles are valuable additions to the DREADD toolkit. The combination of CAG promoter and fusion protein for somatodendritic targeting of hM3Dq drives robust expression that is readily detected in live and fixed tissue across development. As demonstrated by our experiments, this level of expression is sufficient to non-invasively and dose-dependently manipulate cellular activity in diverse cell types, producing behavioral and physiological changes without undesired phenotypes associated with hM3Dq overexpression. A primary strength of DREADD technology is the ability to manipulate cellular activity in freely moving animals, but this advantage is compromised by strategies that require invasive delivery of the DREADD. For instance, viral injection of deep brain structures can result in significant damage to overlying parenchyma and even death of experimental animals. In contrast, our recombinase-responsive hM3Dq alleles offer a truly non-invasive means to activate genetically defined cells.

These alleles offer several important advantages not shared by published hM3Dq alleles. *RC*::*FL-hM3Dq* offers intersectional genetic control of hM3Dq expression, thus providing increased spatial resolution by precise targeting of hM3Dq to

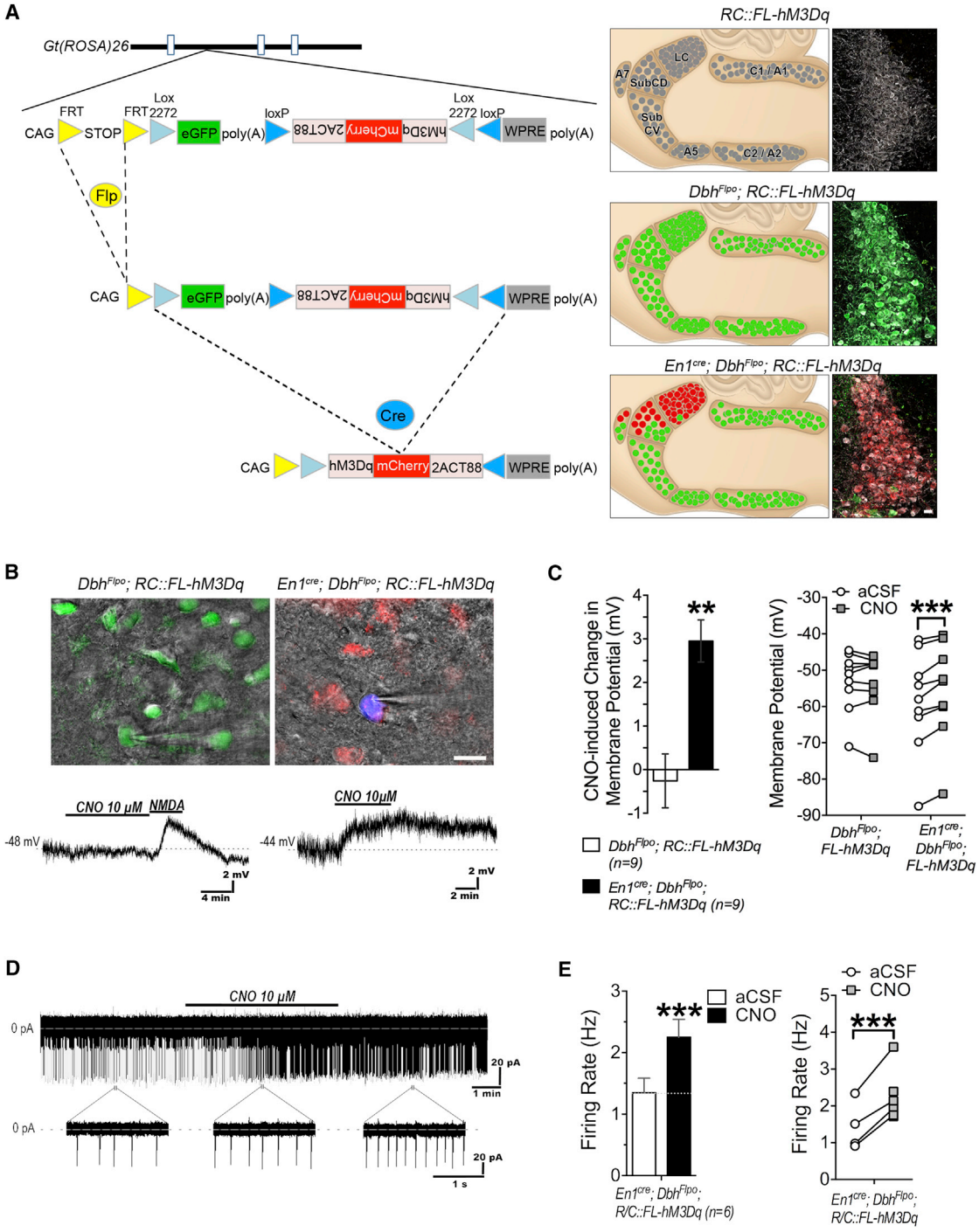

Figure 4. Intersectional Genetic Strategy for Selective, Non-invasive Expression of hM3Dq and Activation of the LC Complex

(A) Schematic diagram of *RC::FL-hM3Dq*, sagittal diagram of noradrenergic nuclei in the hindbrain, and coronal sections through the LC complex immunolabeled for tyrosine hydroxylase (white), EGFP (green), and mCherry (red). Top: in the absence of recombinase expression, noradrenergic neurons are not labeled by EGFP or mCherry. Middle: recombination of *RC::FL-hM3Dq* by Dbh^{Flpo} results in EGFP expression in noradrenergic neurons. Bottom: recombination of *RC::FL-hM3Dq* by $En1^{cre}$ and Dbh^{Flpo} results in hM3Dq-mCherry expression in noradrenergic neurons of the LC complex.

(B) Top: acute hindbrain slices show endogenous expression of EGFP (Dbh^{Flpo}; *RC::FL-hM3Dq*) and hM3Dq-mCherry ($En1^{cre}$; Dbh^{Flpo}; *RC::FL-hM3Dq*) in LC complex neurons patched using Alexa350-filled electrodes (blue). Scale bar, 20 μm. Bottom: representative traces from whole-cell recordings taken from LC neurons with TTX (500 nM) and nimodipine (1 μM) present are shown. Bath application of CNO (10 μM) depolarizes hM3Dq-mCherry+ neurons from resting membrane potential (dashed line). CNO has no effect on membrane potential of EGFP+ neurons, but NMDA (50 μM) does induce depolarization.

(legend continued on next page)

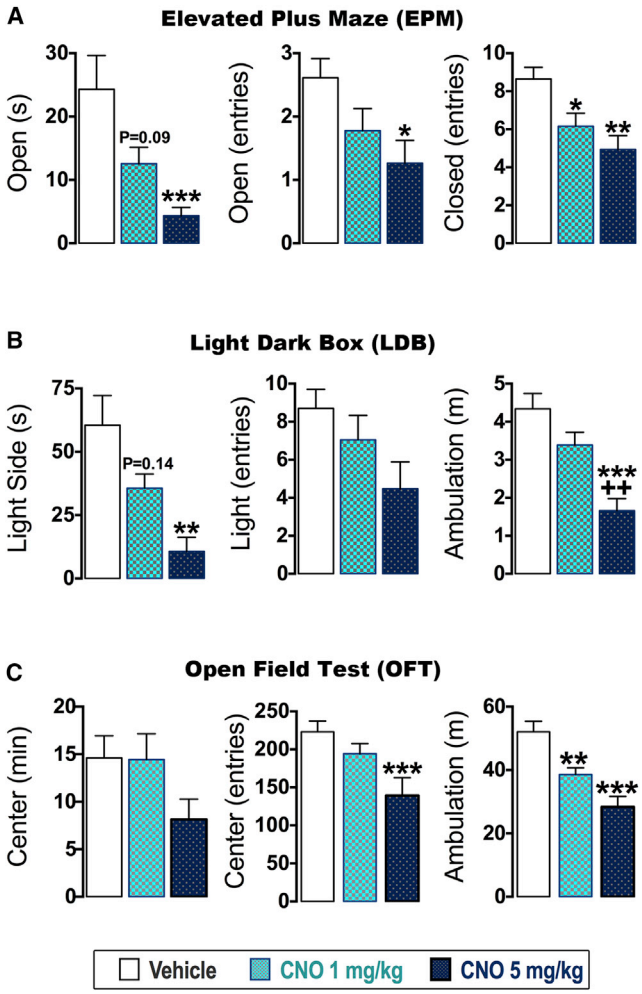

Figure 5. CNO Is Sufficient to Drive Anxiety-like Behavior and Suppress Locomotion in Mice Expressing hM3Dq-mCherry in the LC Complex

(A–C) Behavioral data from elevated plus maze (A, EPM), light-dark box (B, LDB), and open-field test (C, OFT). Data are mean ± SEM for vehicle- (n = 18–21), 1 mg/kg CNO- (n = 16–20), and 5 mg/kg CNO- (n = 13–15) treated *En1*^{cre}; *Dbh*^{Flpo}; *RC*::*FL-hM3Dq* mice (***p < 0.001, **p < 0.01, and *p < 0.05 versus vehicle, Bonferroni; $^{++}$p < 0.01 versus vehicle and 1 mg/kg CNO, Bonferroni). Exact p values list trends for a statistical difference versus vehicle.

cell populations defined by a shared history of Cre and Flp recombinase expression. Unlike existing Cre-responsive hM3Dq knockin alleles (Teissier et al., 2015; Jackson Laboratory Stock 026220, unpublished reagent from U. Hochgeschwender and B. Roth), *RC*::*FL-hM3Dq* and *RC*::*L-hM3Dq* utilize a FLEx switch for efficient control of expression, an mCherry fusion for endogenous fluorescent labeling, and a 2ACT88 epitope for somatodendritic targeting. These features ensure reliable expression of hM3Dq at levels that effectively permit both in vivo visualization and activation of genetically defined cells.

Our characterization of *RC*::*FL-hM3Dq* and *RC*::*L-hM3Dq* demonstrated that somatodendritic expression of hM3Dq can be obtained in virtually any cell population across tissues and developmental stages. We observed the expected expression of mCherry and EGFP, confirming that the FRT-flanked stop cassette and Cre-dependent FLEx switch provide tight recombinase-responsive control of hM3Dq expression. Unexpectedly, we observed ectopic mCherry fluorescence in Cre^{+}, Flp^{-} cerebellar Purkinje cells of *En1*^{cre}; *Dbh*^{Flpo}; *RC*::*FL-hM3Dq* mice. However, our RT-PCR and in vitro electrophysiology experiments unequivocally demonstrated that functional hM3Dq-mCherry is limited to the intersectional population of noradrenergic neurons that share a history of both Flp and Cre expression. Restriction of ectopic mCherry to a single cell type within the broad *En1*^{cre} expression domain suggests that any ectopic fluorescence in other intersectional crosses will be similarly limited and will not interfere with experiments.

We validated the in vivo functional capabilities of *RC*::*FL-hM3Dq* and *RC*::*L-hM3Dq* in three distinct cell types. Activation of hM3Dq expressed bilaterally in the LC complex dose-dependently evoked anxiety-like behavior and suppressed locomotion, consistent with results following unilateral high tonic (5-Hz) optogenetic stimulation of the LC (McCall et al., 2015). The subtle changes in anxiety and locomotion we observed were not obscured by the complete behavioral arrest that was reported following prolonged, high-frequency optogenetic stimulation (>5 Hz) (Carter et al., 2010). Using *RC*::*L-hM3Dq*, we dose-dependently induced gamma oscillations in *Camk2a-cre*+ hippocampal neurons, consistent with results using the tetracycline-controlled *TRE-hM3Dq* transgene (Alexander et al., 2009). Notably, the changes in neural activity we observed were not accompanied by limbic seizures, an extreme phenotype observed using the *TRE-hM3Dq* transgene. Additionally, activation of hM3Dq in *GFAP*+ glia dose-dependently evoked long-lasting changes in body temperature, consistent with prior results (Agulhon et al., 2013).

While all of these phenotypic changes emerged on the timescale of minutes following activation of hM3Dq, their onset differed across experiments. Given that systemically administered CNO is rapidly observed in the brain (Bender et al., 1994), this varied onset of phenotype is likely dependent on the targeted cell type, phenotypic endpoint, and CNO dose employed. Our findings further suggest that levels of hM3Dq expression also influence the onset of phenotype. For example, the hypothermia we observed was slower to emerge than previously described using a *GFAP-hM3Dq* transgene (Agulhon et al.,

(C) Left: average millivolt depolarization by CNO (10 μM) from baseline recorded in hM3Dq-mCherry+ (*En1*^{cre}; *Dbh*^{Flpo}; *RC*::*FL-hM3Dq*, n = 9 cells from seven mice) and EGFP+ (*Dbh*^{Flpo}; *RC*::*FL-hM3Dq*, n = 9 cells from four mice) LC complex neurons (**p < 0.01, t test). Right: population data show the effect of CNO (10 μM) on membrane potential in individual mCherry+ and EGFP+ LC neurons (***p < 0.001, Bonferroni).

(D) Representative trace of cell-attached recordings from an hM3Dq-mCherry+ neuron. Insets of trace show individual firing events in epochs occurring before (left), during (middle), and after (right) superperfusion of CNO. Dashed line indicates the average holding current.

(E) Left: bath application of CNO (10 μM) increases firing rate of hM3Dq-mCherry+ neurons (*En1*^{cre}; *Dbh*^{Flpo}; *RC*::*FL-hM3Dq*, n = 6 cells from three mice). Right: population data show the effect of CNO (10 μM) on firing rate in individual hM3Dq-mCherry+ LC neurons (***p < 0.001, t test).

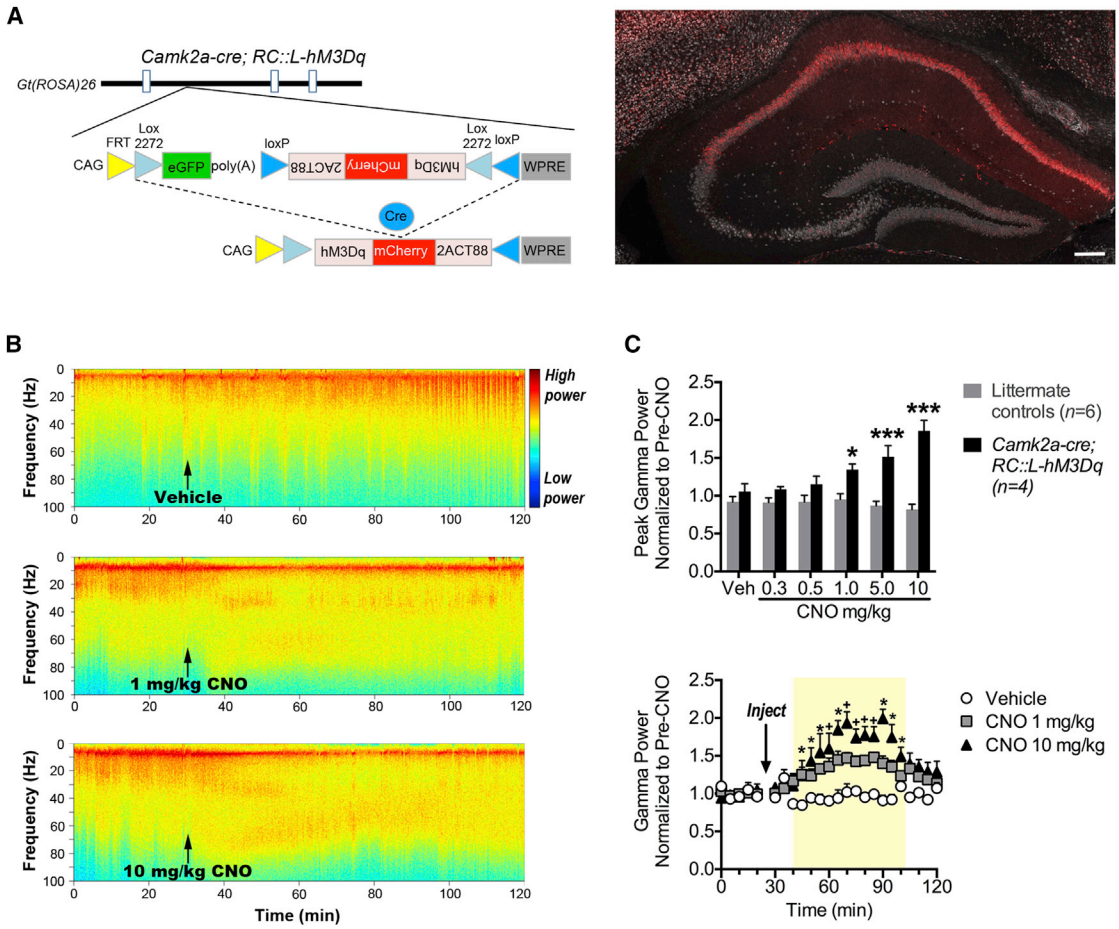

Figure 6. Dose-Dependent Induction of Hippocampal Gamma Oscillations by CNO in Mice Expressing hM3Dq-mCherry in *Camk2a*+ Neurons

(A) Schematic diagram shows Cre-mediated recombination of the FLEx switch permitting hM3Dq-mCherry expression. Coronal section through the hippocampus of a *Camk2a-cre*; *RC::L-hM3Dq* double heterozygote, immunolabeled for mCherry (red) and NeuN (white), is shown. Scale bar, 500 μm.

(B) Spectrograms show frequency composition of local field potentials (LFPs) recorded from *Camk2a-cre*; *RC::L-hM3Dq* mice before, during, and after administration of vehicle or CNO at 1 or 10 mg/kg i.p.

(C) LFP data were divided into 5-min time bins and power spectral densities were computed. Pre-CNO power was the average gamma power (50–80 Hz) across 0–25 min. The 25- to 30-min bin was not included for analysis because mice were handled and injected. Gamma power post-CNO injection was normalized to pre-CNO power. Peak gamma power was averaged across 65- to 80-min bins (i.e., 35–50 min post-CNO) and normalized to pre-CNO. Mice were administered all doses listed. Top: time course of gamma power for vehicle- and CNO-treated *Camk2a-cre*; *RC::L-hM3Dq* double heterozygotes is shown. The yellow window indicates the time period during which CNO increased gamma power (n = 4 mice). Bottom: peak gamma power following CNO injection for *Camk2a-cre*; *RC::L-hM3Dq* and littermate control mice demonstrates dose dependence (***$p < 0.001$ and *$p < 0.05$ versus vehicle, Bonferroni; $^{+}p < 0.05$ versus both CNO 1 mg/kg and vehicle, Bonferroni).

2013). This result, together with the absence of extreme phenotypes like seizures or behavioral arrest in the other crosses, is likely due to lower levels of hM3Dq expression from our single-copy knockin allele compared to transgenic or viral delivery. Taken together, these findings indicate that our hM3Dq alleles modulate cellular activity to produce physiologically relevant changes in behavior without untoward effects that impede or confound interpretation.

In summary, *RC::FL-hM3Dq* and *RC::L-hM3Dq* take full advantage of the power of DREADD technology to non-invasively manipulate cellular activity. Our characterization of these alleles demonstrates their capacity to target genetically defined cell populations, regardless of anatomical location or distribution. In addition, the ability to express hM3Dq at any time point offers the opportunity to uncover the functional consequences of cellular activation throughout development. Together, these capabilities render the hM3Dq alleles broadly useful for controlling the activity of diverse cell types to uncover their function and dysfunction.

EXPERIMENTAL PROCEDURES

Procedures related to the use of mice were conducted according to NIH guidelines and the National Research Council Guide for the Care and Use of Laboratory Animals (Publication 85-23, revised 2013). The Institutional Animal Care and Use Committees (IACUCs) of the NIEHS and University of

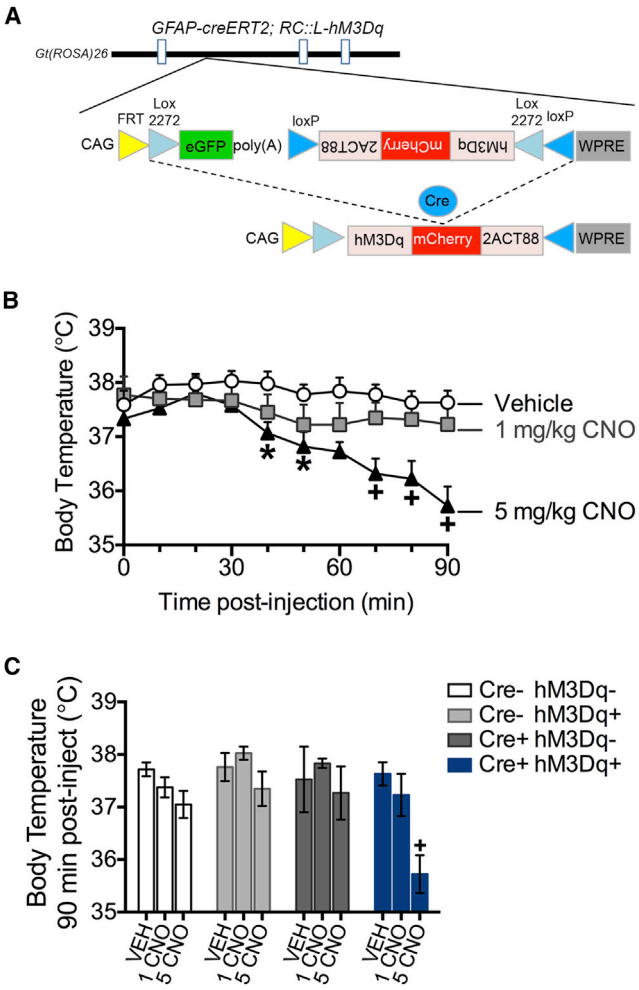

Figure 7. Activation of hM3Dq-mCherry in Glia Is Sufficient to Elicit Hypothermia

(A) Schematic diagram shows Cre-mediated recombination of the FLEx switch permitting hM3Dq-mCherry expression in glia of mice treated with tamoxifen.

(B) Decreased body temperature in *GFAP-creErt2*; *RC*::*L-hM3Dq* double heterozygotes following CNO. Data are mean ± SEM for mice given vehicle (n = 5) or CNO 1 and 5 mg/kg (n = 6) (*p < 0.05 versus vehicle, Bonferroni; $^{+}$p < 0.05 versus vehicle and CNO 1 mg/kg, Bonferroni).

(C) CNO has no effect on the body temperature of littermate controls ($^{+}$p < 0.05 versus vehicle and CNO 1 mg/kg, Bonferroni).

North Carolina approved all experiments. Detailed methods are provided in the Supplemental Experimental Procedures.

Generation of Mouse Lines

To generate our targeting vector for homologous recombination in embryonic stem cells, we first modified a Cre-dependent FLEx switch (Atasoy et al., 2008; Schnütgen et al., 2003) by insertion of an EGFP cDNA and rabbit β-globin polyadenylation cassette between the 5′ lox2272 and loxP sites. We amplified FRT-flanked and rox-flanked His3-SV40 transcriptional stop cassettes, using as the PCR template a pBS302 plasmid (Sauer, 1993) modified to remove the internal MfeI site. The stop cassettes and FLEx switch containing EGFP were then cloned into the *Gt(ROSA)26Sor* targeting vector pRC-RFLTG (Plummer et al., 2015) after digestion with MluI and FseI. The digested fragment of pRC-RFLTG provided a CAG promoter (Niwa et al., 1991), woodchuck hepatitis virus posttranscriptional regulatory element (WPRE) (Zufferey et al., 1999), bGH poly(A) cassette, the 5′ and 3′ homology to the Gt(ROSA)26Sor locus, and attB/attP-flanked Neo cassette. A cDNA encoding the hM3Dq-mCherry-2ACT88 fusion protein, which contains the final 264 coding nucleotides of the rat *Htr2A* gene (Xia et al., 2003), was generously provided by Bryan Roth (University of North Carolina). This cDNA was cloned into the center of the modified FLEx switch, in antisense orientation relative to the CAG promoter and EGFP cDNA, to produce the final targeting vector pRC-RFL-hM3Dq.

Linearized pRC-RFL-hM3Dq was electroporated into G4 embryonic stem cells (George et al., 2007) obtained from the Lunenfeld-Tanenbaum Research Institute, and long-range PCR and Southern blotting identified homologous recombinants. A recombinant clone was transiently transfected with pPGKPhiC31obpa (Raymond and Soriano, 2007) to remove the attb-attp-flanked Neo cassette, and two subclones were injected into B6(Cg)-*Tyr*$^{c-2J}$/J blastocysts to produce chimeric mice. The *RC*::*FL-hM3Dq* strain was established by breeding chimeras with B6;129-*Tg*(*CAG-dre*)*1Afst* mice (Anastassiadis et al., 2009) to excise the rox-flanked stop cassette, and the *RC*::*L-hM3Dq* strain was established by crossing *RC*::*FL-hM3Dq* with B6.Cg-*Tg*(*ACTFlpe*)*9205Dym*/*J* mice (*ACTB-Flpe*) (Rodríguez et al., 2000) to excise the FRT-flanked stop cassette. Both strains were maintained by backcrossing to C57BL/6J mice. *RC*::*FL-hM3Dq* (JAX#026942) and *RC*::*L-hM3Dq* (JAX#026943) mice will be available from the Jackson Laboratory.

Experimental Crosses

To demonstrate ubiquitous expression of EGFP and hM3Dq-mCherry encoded by our DREADD alleles, we crossed *RC*::*FL-hM3Dq* mice with *ACTB-Flpe* followed by B6;FVB-*Tg*(*ACTB-cre*)*2Mrt* (*ACTB-cre*) (Lewandoski et al., 1997). Embryos were collected at embryonic day (E) 11.5, and adult organs were collected from 10-week-old mice. *RC*:*L-hM3Dq* mice were separately crossed with B6(C3)-*Tg*(*GFAP-cre/ERT2*)*13Kdmc* (Casper et al., 2007) and B6.Cg-*Tg*(*Camk2a-cre*)*T29-1Stl* (Tsien et al., 1996) mice. To generate *En1*^{cre}; *Dbh*^{Flpo}; *RC*::*FL-hM3Dq* mice, *RC*::*FL-hM3Dq* mice were first crossed to *B6*;*129-Dbh*$^{tm1(Flpo)Pjen}$ (*Dbh*^{Flpo}) heterozygotes (Robertson et al., 2013), and offspring were backcrossed to generate animals heterozygous for *Dbh*^{Flpo} and homozygous for *RC*::*FL-hM3Dq*. The mice subsequently were crossed with B6.Cg-*En1*$^{tm2(cre)Wrst}$ (*En1*^{cre}) heterozygotes (Kimmel et al., 2000) to generate *En1*^{cre}; *Dbh*^{Flpo}; *RC*::*FL-hM3Dq* triple heterozygotes.

Tissue Collection and Immunohistochemistry

Embryos were fixed overnight by immersion in 4% paraformaldehyde (PFA) in 0.01 M PBS at 4°C. Adult mice were anesthetized with sodium pentobarbital (0.1 ml of 50 mg/ml i.p.) and perfused transcardially with PBS followed by 4% PFA in PBS. Brains were postfixed overnight by immersion in 4% PFA at 4°C, and then rinsed in PBS before transfer to 30% sucrose in PBS for 48 hr at 4°C. Tissue for immunohistochemistry was embedded in Tissue Freezing Medium (General Data) and sectioned at 40 μm on a Leica CM3050-S cryostat (Leica Biosystems). Free-floating sections were collected for immunolabeling using antibodies described in the Supplemental Experimental Procedures. After staining, sections were mounted on microscope slides and coverslips were attached with Vectashield or Vectashield plus DAPI (Vector Laboratories) before imaging.

Digital Image Processing

Images of native fluorescence in whole embryos and adult brains were collected on a Zeiss SteREO Lumar.V12 stereomicroscope (Carl Zeiss Microscopy). Images of the LC complex from acute slices were acquired using a Zeiss Axio Examiner microscope and camera (Axiocam 503) equipped with Zen 2012 Blue Software (Carl Zeiss). The images of acute slices were processed with ImageJ software (NIH) by merging color channels, adjusting brightness and contrast, and applying a smoothing filter. Images of immunofluorescent-labeled sections were collected on a Zeiss LSM 710, 780, or 880 inverted confocal microscope. Zen 2012 Black Software (Carl Zeiss) was used to convert z stacks to maximum-intensity projections. Images were modified only by brightness and contrast adjustments to optimize the full dynamic range of the fluorescence signal. Anatomical location was confirmed by reference to a mouse brain atlas (Paxinos and Franks, 2013).

Slice Electrophysiology

Following anesthesia of *En1*^{cre}; *Dbh*^{Flpo}; *RC*::*FL-hM3Dq* and littermate mice, coronal hindbrain slices (250 μm) were cut in ice-cold cutting solution and incubated at 28–30°C in oxygenated artificial cerebrospinal fluid (aCSF) for at least 30 min. All solutions are listed in the Supplemental Experimental Procedures. Slices were transferred to a recording chamber and perfused with aCSF (32°C) at 2 ml/min. Patch electrodes (1–5 MΩ) were pulled from borosilicate glass. To determine whether CNO (10 μM) would alter membrane potential, whole-cell current-clamp recordings were made from EGFP+ and hM3Dq-mCherry+ LC neurons in the presence of TTX (500 nM) and nimodipine (1 μM). To confirm the absence of functional hM3Dq, recordings were similarly made from mCherry+ cerebellar Purkinje cells. Cell-attached voltage-clamp recordings also were made from hM3Dq-mCherry+ LC neurons to quantify the increase in firing events elicited by CNO (10 μM). Data were collected at 10 kHz using an EPC 800 amplifier (HEKA) and DigiData 132x digitizer (Molecular Devices). Analyses were performed in ClampFit 10.4 on traces that were filtered at 3 Hz (voltage traces) or 1 Hz (current traces).

Anxiety-like Behavior

En1^{cre}; *Dbh*^{Flpo}; *RC*::*FL-hM3Dq* and littermate mice were randomly assigned to receive two i.p. injections of vehicle or CNO (1 or 5 mg/kg). Mice received the first injection immediately before the OFT, and the second injection was 2–3 days later, ~15 min before the LDB. Mice were tested in the EPM directly after the LDB. Details of the tests are described below and in the Supplemental Experimental Procedures.

OFT

Mice were placed in an open arena (27 × 27 × 20 cm, Med Associates) that was not illuminated (0 lux). Exploration in the center (14.3 × 14.3 cm) and remaining periphery of the arena was measured for 90 min.

LDB

Mice were allowed to freely explore an arena (27 × 27 × 20 cm, Med Associates) that was divided into two equal compartments. Exploration in the dark (0 lux) and light (~950 lux) compartments of the arena was measured for 10 min.

EPM

Mice were placed on a plus-shaped maze that was brightly illuminated (300 lux) and elevated 20 in. Exploration in the open (11 × 2 in) and closed (11 × 2 × 5 in) arms of the maze was measured for 5 min, as previously described (Sciolino et al., 2015).

In Vivo Electrophysiology

A ten-channel array (44-μm polyimide-coated steel wires, Sandvic), soldered to circuit board (San Francisco Circuits) and connector (Omnetics), was implanted into the hippocampus of anesthetized *Camk2a-cre*; *RC*::*L-hM3Dq* and littermate control mice using the following stereotaxic coordinates (mm): −2.06 anteroposterior, 2.1 mediolateral, and 2.1 dorsoventral from bregma (Paxinos and Franks, 2013). Local field potentials were recorded using a 32-channel wireless headstage (Triangle BioSystems International) and Cerebus acquisition system (Blackrock Microsystems). During recordings, mice were placed in a plexiglass chamber (20 × 20 in) and given an i.p. injection of vehicle or the following escalating doses of CNO: 0.03, 0.1, 0.3, 0.5, 1, 5, and 10 mg/kg, as previously described (Alexander et al., 2009). All mice received each dose of CNO with 2–3 days between treatments. Analyses were performed in MATLAB R2014a (MathWorks) using Chronux software on traces that were band-pass filtered (0.3–500 Hz) and stored at 1 kHz. Details are provided in the Supplemental Experimental Procedures.

Tamoxifen Dosing

Tamoxifen (T5648, Sigma-Aldrich) was dissolved in 10:1 corn oil:ethanol at a concentration of 20 mg/ml (w/v). To induce Cre-mediated recombination, *GFAP-creERT2*; *RC*::*L-hM3Dq* double heterozygous mice and littermate controls received daily doses of tamoxifen (100 mg/kg i.p., 0.05 ml/10 g body weight) for 5 days during postnatal weeks 6–12.

Body Temperature

Tamoxifen-treated *GFAP-creErt2*; *RC*::*L-hM3Dq* and littermate mice were briefly restrained for baseline measurement of body temperature using a rectal probe. Following i.p. injection of vehicle or CNO (1 or 5 mg/kg), body temperature was measured in 10-min intervals for 90 min. A heating pad was provided to hypothermic mice after testing. All mice were tested twice with at least 5 days of recovery between the tests.

Data Analysis and Statistics

All data are reported as mean ± SEM. Datasets met normality (Shapiro-Wilk test) and equal variance (Levine test) assumptions. Differences between groups were determined using t tests or ANOVA. Bonferroni post hoc tests were performed when necessary to correct for multiple comparisons. Significance for all analyses was set to $p < 0.05$. Analyses were performed using GraphPad Prism 6.0, MATLAB R2014a, and IBM SPSS 21.0. Details for the analyses are described in the Supplemental Experimental Procedures.

SUPPLEMENTAL INFORMATION

Supplemental Information includes Supplemental Experimental Procedures, seven figures, and one table and can be found with this article online at http://dx.doi.org/10.1016/j.celrep.2016.05.034.

AUTHOR CONTRIBUTIONS

N.W.P. and P.J. conceived the project and designed the *RC*::*FL-hM3Dq* and *RC*::*L-hM3Dq* lines. N.W.P. generated the targeting vector. N.R.S., N.W.P., Y.-W.C., S.D.R., and P.J. characterized the mouse lines. N.R.S. and Z.A.M. performed the slice recordings. N.R.S. and P.J. conducted the behavioral tests. G.M.A. performed in vivo electrophysiology with assistance from N.R.S. S.M.D. supported G.M.A. Y.-W.C. and P.J. performed the temperature recordings. N.R.S., Y.-W.C., G.M.A., and Z.A.M. performed statistical data analysis. N.R.S., N.W.P., and P.J. wrote the manuscript with input from co-authors.

ACKNOWLEDGMENTS

We thank D. D'Agostin, G. Jones, and K. Smith for technical assistance. We thank B. Roth (University of North Carolina) for providing the hM3Dq-mCherry-2ACT88 cDNA. We also thank J. Haam, C. Erxleben, C. Hull (Duke University), and D. Weinshenker (Emory University) for helpful advice. Valuable support was provided by the NIEHS Comparative Medicine Branch, Knockout Mouse Core, Biostatistics and Computational Biology Branch, and Fluorescence Microscopy and Imaging Core. We thank the NIDA Drug Supply Program for providing the CNO. This research was supported by the Intramural Research Program of the NIH, NIEHS (ES102805 to P.J. and ES100221 to S.M.D.).

Received: February 4, 2016
Revised: April 5, 2016
Accepted: May 6, 2016
Published: June 2, 2016

REFERENCES

Agulhon, C., Boyt, K.M., Xie, A.X., Friocourt, F., Roth, B.L., and McCarthy, K.D. (2013). Modulation of the autonomic nervous system and behaviour by acute glial cell Gq protein-coupled receptor activation in vivo. J. Physiol. *591*, 5599–5609.

Alexander, G.M., Rogan, S.C., Abbas, A.I., Armbruster, B.N., Pei, Y., Allen, J.A., Nonneman, R.J., Hartmann, J., Moy, S.S., Nicolelis, M.A., et al. (2009). Remote control of neuronal activity in transgenic mice expressing evolved G protein-coupled receptors. Neuron *63*, 27–39.

Anastassiadis, K., Fu, J., Patsch, C., Hu, S., Weidlich, S., Duerschke, K., Buchholz, F., Edenhofer, F., and Stewart, A.F. (2009). Dre recombinase, like Cre, is a highly efficient site-specific recombinase in E. coli, mammalian cells and mice. Dis. Model. Mech. *2*, 508–515.

Armbruster, B.N., Li, X., Pausch, M.H., Herlitze, S., and Roth, B.L. (2007). Evolving the lock to fit the key to create a family of G protein-coupled receptors

potently activated by an inert ligand. Proc. Natl. Acad. Sci. USA *104*, 5163–5168.

Atasoy, D., Aponte, Y., Su, H.H., and Sternson, S.M. (2008). A FLEX switch targets Channelrhodopsin-2 to multiple cell types for imaging and long-range circuit mapping. J. Neurosci. *28*, 7025–7030.

Bender, D., Holschbach, M., and Stöcklin, G. (1994). Synthesis of n.c.a. carbon-11 labelled clozapine and its major metabolite clozapine-N-oxide and comparison of their biodistribution in mice. Nucl. Med. Biol. *21*, 921–925.

Carter, M.E., Yizhar, O., Chikahisa, S., Nguyen, H., Adamantidis, A., Nishino, S., Deisseroth, K., and de Lecea, L. (2010). Tuning arousal with optogenetic modulation of locus coeruleus neurons. Nat. Neurosci. *13*, 1526–1533.

Casper, K.B., Jones, K., and McCarthy, K.D. (2007). Characterization of astrocyte-specific conditional knockouts. Genesis *45*, 292–299.

de Oliveira, R.B., Howlett, M.C., Gravina, F.S., Imtiaz, M.S., Callister, R.J., Brichta, A.M., and van Helden, D.F. (2010). Pacemaker currents in mouse locus coeruleus neurons. Neuroscience *170*, 166–177.

Friedrich, G., and Soriano, P. (1991). Promoter traps in embryonic stem cells: a genetic screen to identify and mutate developmental genes in mice. Genes Dev. *5*, 1513–1523.

George, S.H., Gertsenstein, M., Vintersten, K., Korets-Smith, E., Murphy, J., Stevens, M.E., Haigh, J.J., and Nagy, A. (2007). Developmental and adult phenotyping directly from mutant embryonic stem cells. Proc. Natl. Acad. Sci. USA *104*, 4455–4460.

Kimmel, R.A., Turnbull, D.H., Blanquet, V., Wurst, W., Loomis, C.A., and Joyner, A.L. (2000). Two lineage boundaries coordinate vertebrate apical ectodermal ridge formation. Genes Dev. *14*, 1377–1389.

Lewandoski, M., Meyers, E.N., and Martin, G.R. (1997). Analysis of Fgf8 gene function in vertebrate development. Cold Spring Harb. Symp. Quant. Biol. *62*, 159–168.

McCall, J.G., Al-Hasani, R., Siuda, E.R., Hong, D.Y., Norris, A.J., Ford, C.P., and Bruchas, M.R. (2015). CRH Engagement of the Locus Coeruleus Noradrenergic System Mediates Stress-Induced Anxiety. Neuron *87*, 605–620.

Niwa, H., Yamamura, K., and Miyazaki, J. (1991). Efficient selection for high-expression transfectants with a novel eukaryotic vector. Gene *108*, 193–199.

Paxinos, G., and Franks, K.B.J. (2013). The mouse brain in sterotaxic coordinates (San Diego: Academic Press).

Plummer, N.W., Evsyukova, I.Y., Robertson, S.D., de Marchena, J., Tucker, C.J., and Jensen, P. (2015). Expanding the power of recombinase-based labeling to uncover cellular diversity. Development *142*, 4385–4393.

Raymond, C.S., and Soriano, P. (2007). High-efficiency FLP and PhiC31 site-specific recombination in mammalian cells. PLoS ONE *2*, e162.

Robertson, S.D., Plummer, N.W., de Marchena, J., and Jensen, P. (2013). Developmental origins of central norepinephrine neuron diversity. Nat. Neurosci. *16*, 1016–1023.

Rodríguez, C.I., Buchholz, F., Galloway, J., Sequerra, R., Kasper, J., Ayala, R., Stewart, A.F., and Dymecki, S.M. (2000). High-efficiency deleter mice show that FLPe is an alternative to Cre-loxP. Nat. Genet. *25*, 139–140.

Sauer, B. (1993). Manipulation of transgenes by site-specific recombination: use of Cre recombinase. Methods Enzymol. *225*, 890–900.

Schnütgen, F., Doerflinger, N., Calléja, C., Wendling, O., Chambon, P., and Ghyselinck, N.B. (2003). A directional strategy for monitoring Cre-mediated recombination at the cellular level in the mouse. Nat. Biotechnol. *21*, 562–565.

Sciolino, N.R., Smith, J.M., Stranahan, A.M., Freeman, K.G., Edwards, G.L., Weinshenker, D., and Holmes, P.V. (2015). Galanin mediates features of neural and behavioral stress resilience afforded by exercise. Neuropharmacology *89*, 255–264.

Sonner, J.M., Cascio, M., Xing, Y., Fanselow, M.S., Kralic, J.E., Morrow, A.L., Korpi, E.R., Hardy, S., Sloat, B., Eger, E.I., 2nd, and Homanics, G.E. (2005). Alpha 1 subunit-containing GABA type A receptors in forebrain contribute to the effect of inhaled anesthetics on conditioned fear. Mol. Pharmacol. *68*, 61–68.

Teissier, A., Chemiakine, A., Inbar, B., Bagchi, S., Ray, R.S., Palmiter, R.D., Dymecki, S.M., Moore, H., and Ansorge, M.S. (2015). Activity of Raphé Serotonergic Neurons Controls Emotional Behaviors. Cell Rep. *13*, 1965–1976.

Tsien, J.Z., Chen, D.F., Gerber, D., Tom, C., Mercer, E.H., Anderson, D.J., Mayford, M., Kandel, E.R., and Tonegawa, S. (1996). Subregion- and cell type-restricted gene knockout in mouse brain. Cell *87*, 1317–1326.

Urban, D.J., and Roth, B.L. (2015). DREADDs (designer receptors exclusively activated by designer drugs): chemogenetic tools with therapeutic utility. Annu. Rev. Pharmacol. Toxicol. *55*, 399–417.

Williams, J.T., North, R.A., Shefner, S.A., Nishi, S., and Egan, T.M. (1984). Membrane properties of rat locus coeruleus neurones. Neuroscience *13*, 137–156.

Xia, Z., Hufeisen, S.J., Gray, J.A., and Roth, B.L. (2003). The PDZ-binding domain is essential for the dendritic targeting of 5-HT2A serotonin receptors in cortical pyramidal neurons in vitro. Neuroscience *122*, 907–920.

Zhu, H., and Roth, B.L. (2014). DREADD: a chemogenetic GPCR signaling platform. Int. J. Neuropsychopharmacol. *18*, pyu007.

Zufferey, R., Donello, J.E., Trono, D., and Hope, T.J. (1999). Woodchuck hepatitis virus posttranscriptional regulatory element enhances expression of transgenes delivered by retroviral vectors. J. Virol. *73*, 2886–2892.

Cell Reports, Volume *15*

Supplemental Information

Recombinase-Dependent Mouse Lines for Chemogenetic Activation of Genetically Defined Cell Types

Natale R. Sciolino, Nicholas W. Plummer, Yu-Wei Chen, Georgia M. Alexander, Sabrina D. Robertson, Serena M. Dudek, Zoe A. McElligott, and Patricia Jensen

SUPPLEMENTAL INFORMATION

Figure S1

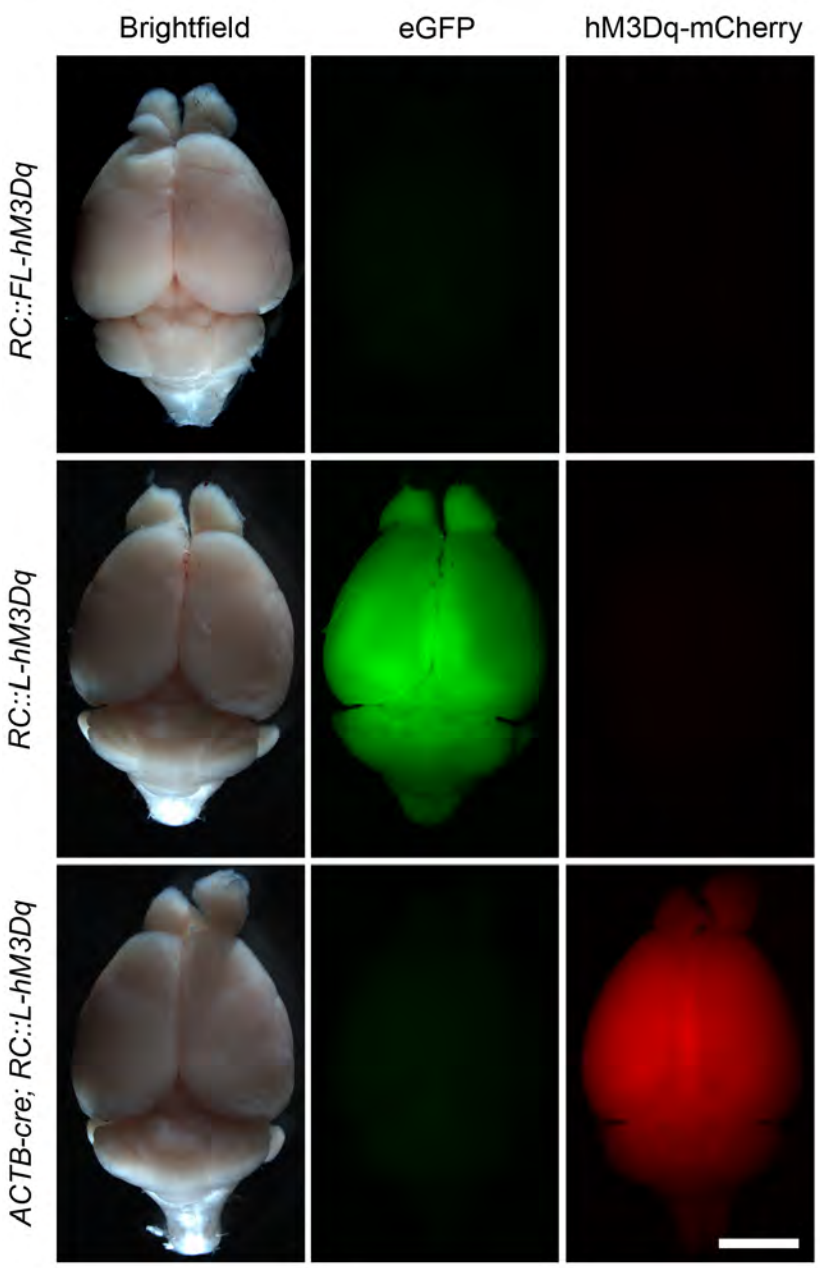

Figure S1. Universal Alleles *RC::FL-hM3Dq* and *RC::L-hM3Dq* Permit Conditional Expression of hM3Dq-mCherry and EGFP in the Adult Brain (Related to Figure 1)

(Top) In adult *RC::FL-hM3Dq* heterozygous brain, no EGFP or hM3Dq-mCherry is observed in the absence of recombinase.

(Middle) Ubiquitous expression of EGFP, but not hM3Dq-mCherry, is observed in adult *RC::L-hM3Dq* heterozygous brain.

(Bottom): Germline expression of Cre recombinase results in ubiquitous expression of hM3Dq-mCherry in adult *ACTB-cre; RC::L-hM3Dq* brain. Images show native fluorescence. Scale bar: 7 mm.

Figure S2

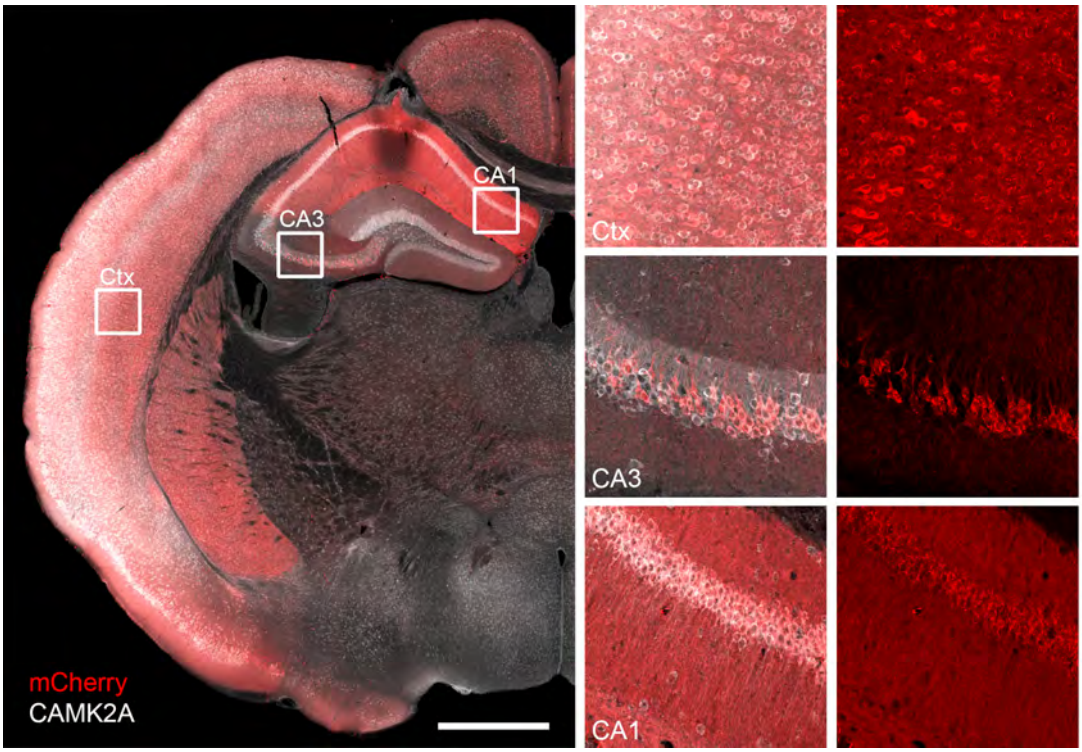

Figure S2: Targeting of hM3Dq-mCherry to CAMK2+ Neurons (Related to Figure 3)
Coronal section of a *Camk2a-cre; RC::L-hM3Dq* brain immunolabeled for mCherry (red) and CAMK2A (white). Boxes on the low-magnification image (left) show the location of magnified images. The magnified images show merged mCherry/CAMK2A co-localization (right) or mCherry alone (far right). Consistent with the known expression pattern of the *Camk2a-cre* transgene (Sonner et al., 2005), mCherry is expressed in a large subset of CAMK2A neurons in the cortex (Ctx) and hippocampal CA1, and in scattered cells of other hippocampal regions (CA3 shown). Scale bar: 2000 µm or 165 µm (magnified images).

Figure S3

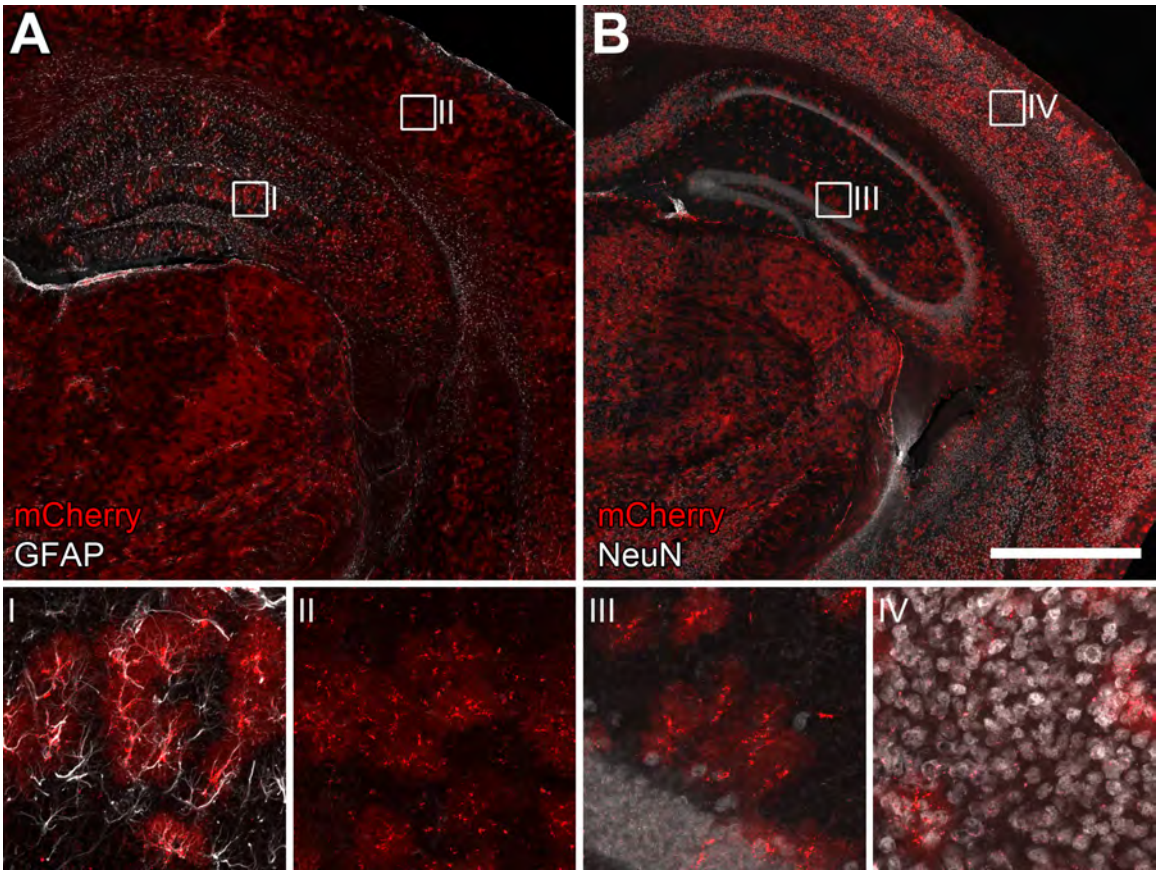

Figure S3: Targeting of hM3Dq-mCherry to GFAP+ Glia (Related to Figure 3)
(A) Coronal section of a tamoxifen-treated *GFAP-creERT2; RC::L-hM3Dq* brain immunolabeled for mCherry (red) and the glial marker GFAP (white). Boxes indicate the location of magnified images (I, II). At higher magnification, astrocytes are observed co-labeled with mCherry and GFAP (I). Consistent with known variability in astrocytic GFAP expression and immunolabeling (Sofroniew and Vinters, 2010), mCherry+ glia in some areas (II) are not GFAP immunoreactive.
(B) Coronal section of a tamoxifen-treated *GFAP-creERT2; RC::L-hM3Dq* brain immunolabeled for mCherry (red) and the neuronal marker NeuN (white) confirms that mCherry is not expressed in neurons. Boxes indicate the location of magnified images (III, IV). The spatial distribution of mCherry-labeled cells does not match that of NeuN-labeled nuclei, indicating that hM3Dq-mCherry is not expressed in neurons. Scale bar: 1000 µm or 110 µm (magnified images).

Figure S4

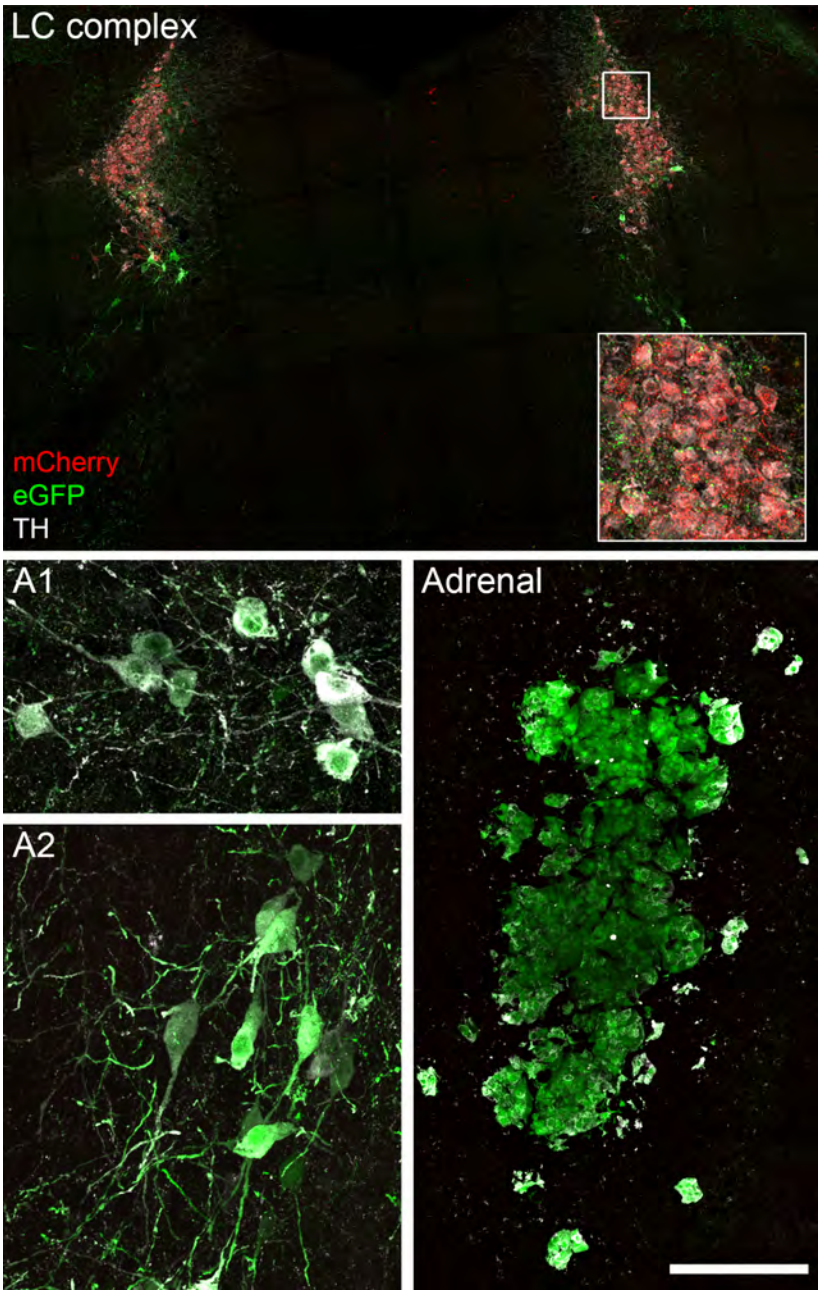

Figure S4: Targeting of hM3Dq-mCherry to the Noradrenergic LC Complex (Related to Figure 3)
Noradrenergic/adrenergic cells of the LC complex, A1, and A2 nuclei in the brainstem and the adrenal medulla of an *En1^{cre}; Dbh^{Flpo}; RC::FL-hM3Dq* mouse immunolabeled for mCherry (red), EGFP (green), and tyrosine hydroxylase (white).
(Top) In the LC complex, mCherry is restricted to noradrenergic neurons (TH+) that have a history of both *En1^{cre}* and *Dbh^{Flpo}* expression (Robertson et al., 2013). Noradrenergic neurons in the dorsal subcoeruleus that originate outside the *En1* expression domain are labeled with EGFP. Non-noradrenergic neurons surrounding the bilateral LC complex are unlabeled. Box indicates the location of magnified inset.
(Bottom) Noradrenergic/adrenergic cells (TH+) in the A1 and A2 brainstem nuclei and adrenal medulla expressing *Dbh^{Flpo}*, but not *En1^{cre}*, are labeled with EGFP and do not express hM3Dq-mCherry. Scale bar: 500 µm (LC complex), 105 µm (LC complex inset), 72 µm (A1 and A2), or 180 µm (adrenal).

Figure S5

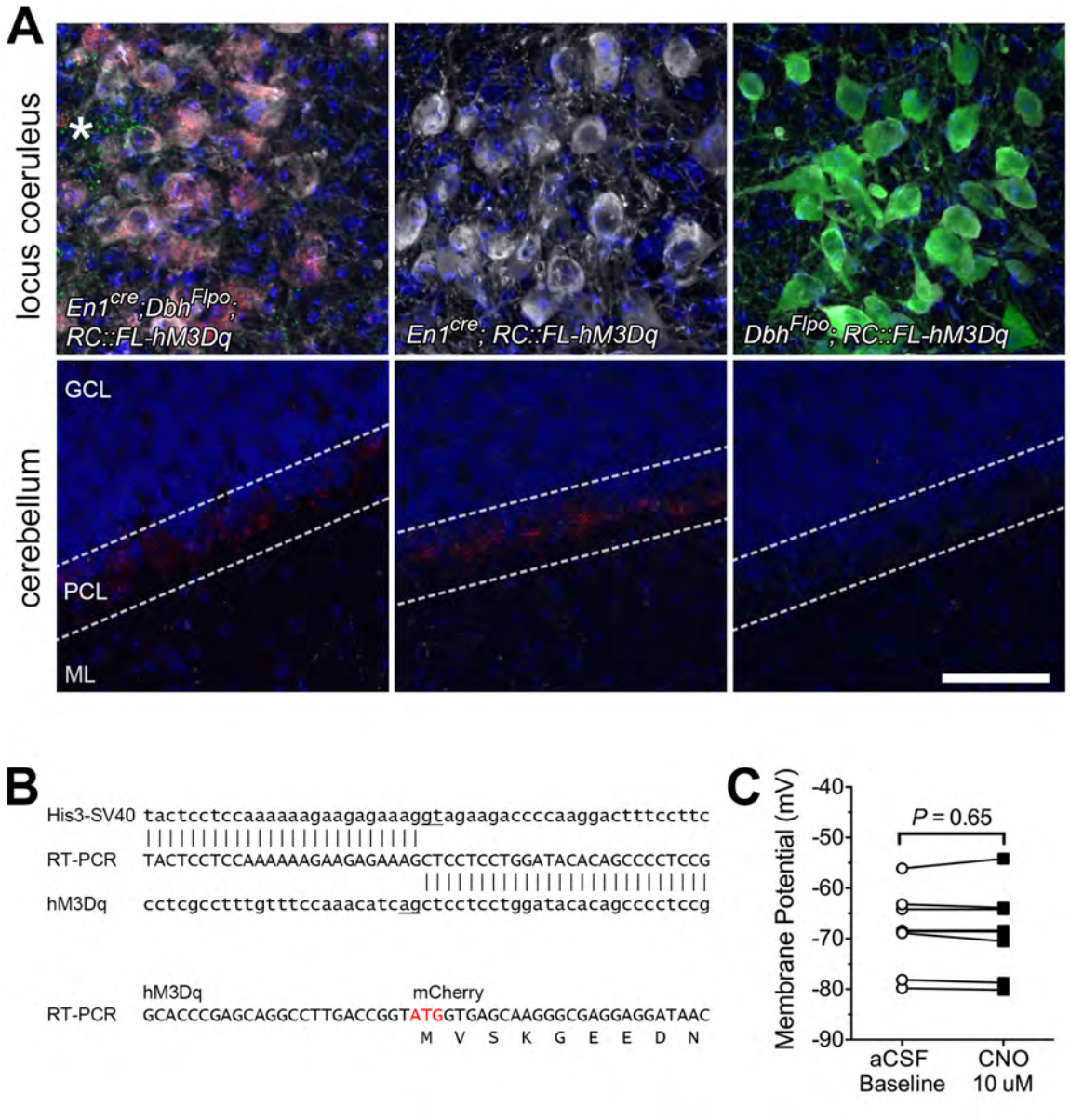

Figure S5. Non-Functional, Ectopic mCherry Fluorescence in Purkinje Cells Observed Following Cre Recombination of *RC::FL-hM3Dq* (Related to Figure 4)

(A) Coronal sections of the locus coeruleus and cerebellum stained for DAPI (blue) and immunolabeled for tyrosine hydroxylase (white), mCherry (red), and EGFP (green). *Left:* In *En1^{cre}; Dbh^{Flpo}; RC::FL-hM3Dq* triple heterozygotes, mCherry and EGFP are observed in noradrenergic locus coeruleus neurons and innervating fibers from other noradrenergic nuclei (asterisk), respectively. Purkinje cells express mCherry, but not EGFP. *Middle*: In *En1^{cre}; RC::FL-hM3Dq* double heterozygotes, locus coeruleus neurons are unlabeled, but Purkinje cells express mCherry. *Bottom:* In *Dbh^{Flpo}; RC::FL-hM3Dq* double heterozygotes, locus coeruleus neurons are labeled with EGFP and Purkinje neurons are unlabeled. GCL, granular cell layer; PCL, Purkinje cell layer; ML, molecular layer. Scale bar: 50 µm.

(B) Sequence from the major RT-PCR product from *En1^{cre}; Dbh^{Flpo}; RC::FL-hM3Dq* cerebellum (uppercase). *Top:* Alignment to His3-SV40 stop cassette and hM3Dq reveals an mRNA splice extending from the middle of the FRT-flanked stop cassette to a cryptic splice acceptor within the hM3Dq cDNA,

eliminating the first 77 nucleotides of hM3Dq. GT and AG dinucleotides of the splice donor and acceptor are underlined. The His3-SV40 sequence and orientation of hM3Dq indicate that the mRNA comes from cells that have expressed Cre but not Flp. *Bottom:* At the site of hM3Dq-mCherry fusion, a start codon (ATG) will permit translation of mCherry without hM3Dq.
(C) CNO (10 μm) has no effect on membrane potential of mCherry-labeled Purkinje cells (*N*=8 cells from 5 mice) from *En1*^{cre}*; Dbh*^{Flpo}*; RC::FL-hM3Dq* triple heterozygotes (Paired *t*-test).

Figure S6

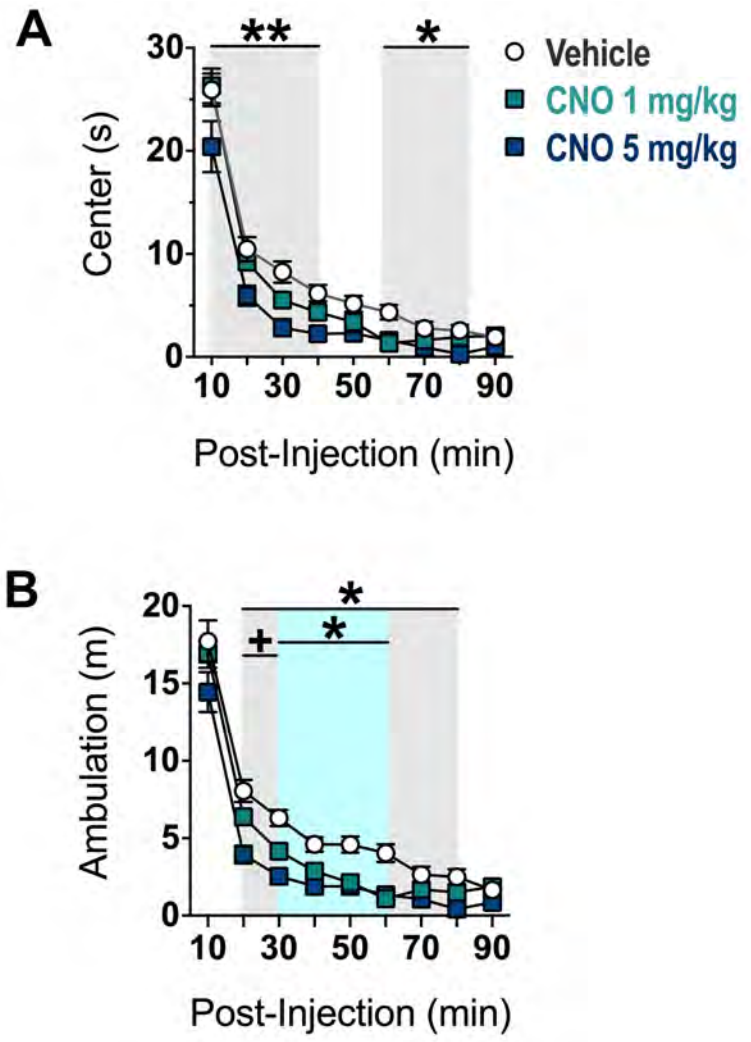

Figure S6: Time Course of Anxiety-like Behavior and Locomotor Suppression of *En1^{cre}; Dbh^{Flpo}; RC::FL-hM3Dq* Mice in the Open Field is Dependent on the Dose of CNO (Related to Figure 5)

(A) The 5-mg/kg dose of CNO reduced center time at 10-40 and 60-80 minutes post-injection compared to vehicle (gray areas on graph). However, center time was not altered by the 1-mg/kg dose of CNO across the experiment. **p<0.01, *p<0.05 vs. Vehicle (Bonferroni).

(B) The 5-mg/kg dose of CNO significantly reduced ambulation 20-80 minutes post-injection compared to vehicle (gray area on graph). The 1-mg/kg dose of CNO also reduced ambulation 30-60 minutes post-injection (blue area on graph). However, the 5-mg/kg CNO dose produced a greater reduction in ambulation compared to the 1-mg/kg dose only during 20-30 minutes post-injection (gray area denoted by +). Data are ± SEM for vehicle (n=18-20), CNO 1 mg/kg (n=16-18), and CNO 5 mg/kg (n=15) treated *En1^{cre}; Dbh^{Flpo}; RC::FL-hM3Dq* triple heterozygous mice tested in the open field. *p<0.05 vs. Vehicle (Bonferroni). +p<0.05 vs. CNO 1 mg/kg (Bonferroni).

Figure S7

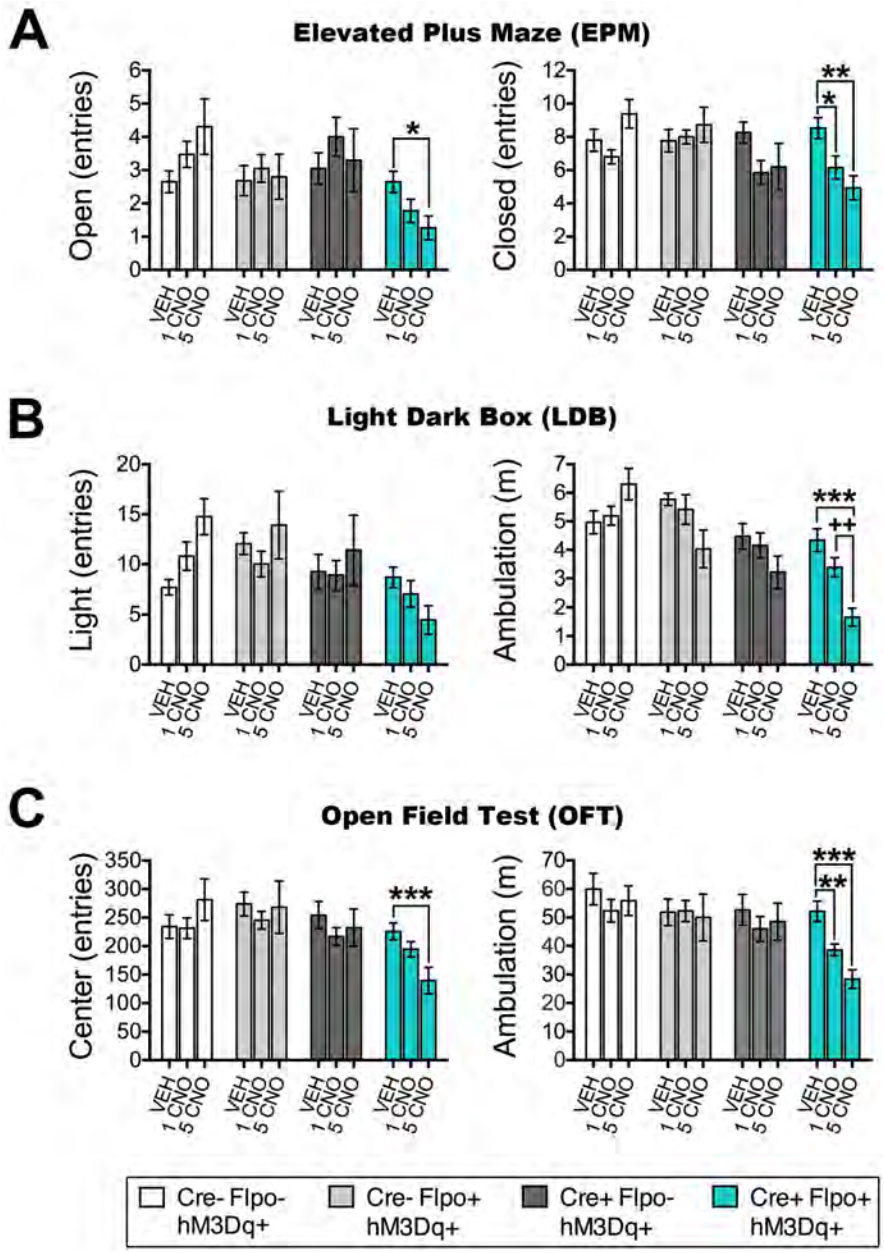

Figure S7. CNO Elicits Anxiety and Hypo-Locomotion Exclusively in *En1^{cre}; Dbh^{Flpo}; RC::FL-hM3Dq* Triple Heterozygotes (Related to Figure 5)

Behavioral data from elevated plus maze (A), light-dark box (B), and open field test (C). CNO evokes anxiety-like behavior and suppresses locomotion specifically in *En1^{cre}; Dbh^{Flpo}; RC::FL-hM3Dq* mice (Cre+ Flp+). CNO has no effect in littermate controls expressing *RC::FL-hM3Dq* (Cre- Flp), *Dbh^{Flpo}; RC::FL-hM3Dq* (Cre- Flp+) or *En1^{cre}; RC::FL-hM3Dq* (Cre+ Flp-). Data are Mean ± SEM Group sizes are as follows: Vehicle treated Flpo-Cre- (n=17-20), Flpo+Cre- (n=16-21), Flpo-Cre+ (n=17-19), and Flpo+Cre+ (n=17-21); CNO 1-mg/kg treated Flpo-Cre- (n=19-21), Flpo+Cre- (n=19), Flpo-Cre+ (n=18-20), and Flpo+Cre+ (n=16-20); CNO 5-mg/kg treated Flpo-Cre-(n=12-13), Flpo+Cre- (n=10-11), Flpo-Cre+ (n=10-11), and Flpo+Cre+ (n=15). ***p<0.001, **p<0.01, *p<0.05 vs. Vehicle (Bonferroni). $^{++}$p<0.01 vs. CNO 1 mg/kg (Bonferroni).

Table S1: Statistics and Sample Sizes of Behavioral Tests (Related to Figures 4, Figure S5, Figure S6)

See Excel File.

SUPPLEMENTAL EXPERIMENTAL PROCEDURES

Antibodies

mCherry-expressing cells were detected with either rabbit anti-mCherry primary antibody (1:20,000; Cat.# ab167453, Abcam, Cambridge MA) and Alexa Fluor 568 goat anti-rabbit secondary antibody (1:1000; Cat.# A11036, Thermo Fisher), or rat anti-mCherry primary antibody (1:1000; Cat.# M11217, Thermo Fisher, Waltham, MA) and Alexa Fluor 568 goat anti-rat secondary antibody (1:1000; Cat.# A11077, Thermo Fisher). EGFP-expressing cells were detected with chicken anti-GFP primary antibody (1:10,000; Cat.# ab13970, Abcam) and Alexa Fluor 488 goat anti-chicken secondary antibody (1:1000; Cat.# A11039, Thermo Fisher). Tyrosine hydroxylase-expressing noradrenergic/adrenergic and dopaminergic neurons were detected with rabbit anti-TH (1:1000, Cat.# AB152, Millipore) and Alexa Fluor 633 goat anti-rabbit secondary antibody (1:1000; Cat.# A21071, Thermo Fisher). *Camk2a*-expressing neurons were detected using rabbit anti-CAMK2A (1/250; Cat.# ab131468, Abcam) and Alexa Fluor 633 goat anti-rabbit secondary antibody (1:1000; Cat.# A21071; Thermo Fisher) after antigen retrieval was performed by boiling sections in water for three minutes, followed by incubation in 0.3% Triton X100 for 15 minutes at room temperature. *Gfap*-expressing glia were detected with mouse anti-GFAP primary antibody (1:1000, Cat.# MAB360, Millipore, Billerica, MA) and Alexa Fluor 633 goat anti-mouse secondary antibody (1:1000; Cat.# A21136, Thermo Fisher). NeuN-expressing neurons were detected using mouse anti-NeuN primary antibody (1:1000, Cat.# MAB377, Millipore) and Alexa Fluor 633 goat anti-mouse secondary antibody (1:1000; Cat.# A21136, Thermo Fisher).

Slice Electrophysiology

*Acute Brain Slices***.** For recordings from the LC complex, *En1^{cre}; Dbh^{Flpo}; RC::FL-hM3Dq* and *Dbh^{Flpo}; RC::FL-hM3Dq* mice (N=14, both sexes) were used at 1-3 months of age. For cerebellar Purkinje recordings, *En1^{cre}; Dbh^{Flpo}; RC::FL-hM3Dq* mice (N=8 males) were used at 3-5 months of age. All mice were anesthetized with Pentobarbital and transcardially perfused with chilled (4ºC) and bubbled (95% O_2 and 5% CO_2) high-sucrose, low Na^+ aCSF (sucrose aCSF contained in mM: 182 sucrose, 20 NaCl, 0.5 KCl, 1 $MgCl_2$-$6H_20$, 1.2 NaH_2PO_4-H_20, 26 $NaHCO_3$, 10 glucose). Mice were quickly decapitated and brains were removed and placed in sucrose aCSF. Coronal slices (250 µm) containing the LC complex and/or cerebellum were cut on a VT1200S vibratome (Leica Biosystems, Buffalo Grove, IL) in sucrose aCSF, and incubated for at least 30 min at 28-30ºC in oxygenated aCSF (aCSF that contained in mM: 124 NaCl, 4 KCl, 1.2 $MgSO_4$-$7H_20$, 2 $CaCl_2$-$2H_20$,1 NaH_2PO_4-H_20, 13 $NaHCO_3$, 5 glucose).

General Recording Methods. Slices were transferred to a recording chamber (RC-26G, Warner Instruments, Hamden, CT) and allowed to rest for an additional 30 min while continuously perfused with heated (32ºC), oxygenated aCSF (CL-100 temperature controller and LCS-1 cooling system, Warner Instruments) at 2 mL/min (Peri-Star Pro peristaltic pump, World Precision Instruments, Sarasota, FL). Data were collected at 10 kHz using an EPC 800 amplifier (HEKA Elektronik, Lambrecht, Germany) equipped with DigiData 132x digitizer and pClamp 10.4 software (Molecular Devices, Sunnyvale CA) on a Dell Precision T3610 computer. Patch electrodes were fashioned using borosilicate glass capillary tubing (1.5 mm o.d., 1.12 mm i.d., TW150F-4, World Precision Instruments) pulled by a P97 Flaming Brown microelectrode puller (Sutter, Novato, CA). Neurons were visualized at 40x using a Zeiss Axio Examiner microscope equipped with Axiocam 503 camera (Carl Zeiss Microscopy, Thornwood, NY) and PhotoFluor II light source (89 North, Burlington, VT).

Whole-Cell Recording. Recordings were made from EGFP+ and hM3Dq-mCherry+ neurons of the LC complex, and mCherry+ cerebellar Purkinje cells in current clamp mode. After 5-10 min to allow the baseline to stabilize, membrane potential was recorded in LC neurons before and during bath application of CNO (10 µM, NIDA Drug Supply Program) and then during and after bath application of the positive-control NMDA (50 µM, Sigma, St. Louis, MI). Methods were similar for recordings from mCherry+ cerebellar Purkinje cells, except that membrane potential was recorded before, during, and after bath application of CNO (10 µM). Tip resistance was 3-5 MΩ when electrodes were filled with intracellular solution containing (mM): 135 K Gluc, 5 NaCl, 2 $MgCl_2$-$6H_20$, 10 HEPES, 0.6 EGTA, 4 Na_2ATP, 0.4 Na_2GTP. AlexaFluor 350 dye (Thermo Fisher Scientific) was added to the intracellular solution. Liquid

junction potential was +13 mV and membrane potential was adjusted and reported accordingly.

Cell-Attached Recording. Loose seal recordings (<20 MΩ) were made from hM3Dq-mCherry+ neurons of the LC complex in voltage clamp mode. Traces were monitored for 5-10 minutes to determine whether baseline-firing rate was stable. During this time, a voltage command was applied to shift the baseline to 0 pA to negate current due to a change in the junction potential. Next, firing rate was continuously recorded before, during, and after bath application of CNO (10 μM, NIDA Drug Supply Program). Tip resistance of the recording electrode was 1-3 MΩ when filled with aCSF.

Data Analysis for Slice Electrophysiology. All analyses were performed using ClampFit 10.4 (Molecular Devices). Voltage traces were low-pass filtered at 3 Hz using a Gaussian function, and only recordings with an access resistance of <30 MΩ were included for analysis (Niculescu et al., 2013). Membrane potential was averaged across a recording period of 1 minute (Purkinje recordings) or 2 minutes (LC recordings) within each drug application phase. Each period was selected during the center of each drug phase to avoid inclusion of potential artifact from transition between drugs. LC neurons with resting membrane potentials > -39 mV were excluded to avoid the possibility of including unhealthy cells (e.g., cells damaged during slice preparation) (van den Pol et al., 2002). Only one hM3Dq+ neuron, exhibiting a slight hyperpolarization (by -1.62 mV) during CNO application, was excluded from analysis because it's membrane potential met the outlier criteria (3 SD±Mean). Independent *t*-tests were used to assess whether membrane potential was altered by CNO or recording parameters (TTX vs. TTX+Nimodipine). Two-way ANOVA with Bonferroni follow-up tests were used to determine whether CNO altered membrane potential in a manner dependent on mouse genotype. Current traces were high-pass filtered at 1 Hz, and only LC recordings with a seal resistance of 5-20 MΩ were included for analysis (Nunemaker et al., 2003). Firing rate was averaged across 2-minute periods of recording within each drug application phase. Paired samples t-test was used to determine whether firing rate was altered by CNO.

Drugs for In Vitro Electrophysiology. All stock solutions were diluted in aCSF to final concentration. Stocks of CNO and nimodipine were made in DMSO, and TTX and NMDA were made in ddH_2O. The final volume of DMSO or ddH_2O did not exceed 0.24% or 0.01%.

Anxiety-like Behavior

General Procedure for the Anxiety Test Battery. Male and female (N=210 mice weighing 15-37 g) *En1^{cre}; Dbh^{Flpo}; RC::FL-hM3Dq* and littermate controls were group housed, with *ad libitum* food and water. Mice were housed under a 12:12 light:dark cycle, and were tested in the anxiety test battery during lights ON. Mice were randomly assigned at approximately 2-6 months of age to receive two intraperitoneal (i.p.) injections of vehicle (0.6% DMSO in saline) or clozapine N-oxide (1 or 5 mg/kg.) prior to testing. The first administration of the assigned drug was given immediately before placement in the open field. The second administration was given 2-3 days later, approximately 15 min before the light dark box (LDB) test. Directly after the LDB, Mice were tested in the elevated plus maze (EPM). All injections were administered at 0.1 mL/10 g using drug prepared fresh daily. The experimenter was blind to the assigned drug and genotype for all experiments. Equipment was cleaned between tests using Accel wipes (0.5% Hydrogen Peroxide, AHP Technologies).

Open Field Test (OFT). Mice were placed in the center of an activity monitor box (ENV-510; 27 x 27 x 20 cm, Med Associates) that was enclosed in a sound-attenuated cubicle. For 90 minutes, mice were allowed to freely explore the non-illuminated apparatus (0 lux). Mouse position and movement was tracked by infrared beam breaks measured every 50 milliseconds within the center (14.3 x 14.3 cm) and remaining periphery of the apparatus (SOF-810 version 7, default settings). Ambulation was detected when movement triggered three beam breaks and measured thereafter as distance traveled in continuous (longer than 500 ms) movement outside a 2 by 2 area of x–y beams. Center time and entries are reported as the standard measures of anxiety-like behavior. We also verified that manipulations that changed center exploration had an opposite effect on periphery exploration. Ambulatory distance is reported as an index of locomotion.

Light Dark Box (LDB). The LDB apparatus was divided into a dark (ENV-511; 13.5 x 27 cm) and light side (13.5 x 25 cm). Mice were placed in the light side of the apparatus (ENV-510, Med Associates), and allowed to freely explore both dark (0 lux illumination) and light compartments (~950 lux) for 10 min while behavior was detected automatically by infrared beam breaks (see OFT section for details). Time spent and entries into the light compartment are reported as standard measures of anxiety-like behavior during the last 5 min of the LDB test. This time window corresponds to 20-25 min post-injection, and was selected for analysis to illustrate the anxiogenic effect elicited by CNO, which would otherwise go undetected if data were reported across the entire test duration. Manipulations that changed light chamber exploration were confirmed to have an opposite effect on dark chamber exploration. Ambulatory distance during the last 5 min of the LDB test is reported as the locomotor index.

Elevated Plus Maze (EPM). Directly after LDB testing, mice were placed on a '+' shaped maze standing 20" from floor with a pair of open (11 x 2 inch) and closed arms (11 x 2 x 5 inch) that meet at a central platform (2 x 2 inch). The maze was illuminated at 300 lux. Mice were placed on the center zone facing an open arm and allowed to freely explore for 5 min. Exploration was recorded and analyzed from video by an experimenter blind to genotype and drug treatment. Entrance of all four paws was required to count as a new arm entry (Sciolino et al., 2015). Open arm time and entries are reported as the primary measure of anxiety-like behavior. In addition, manipulations that changed open arm time were also verified to have an opposite effect on closed arm time. Closed arm entries are reported as a proxy of locomotor behavior.

Data Analysis for Anxiety-Related Behavior. To avoid a type II statistical error, Tukey's strategy (1.5 IQR above or below the 25^{th} or 75^{th} percentile) was used for detection and removal of extreme outliers. This conservative strategy identified outliers that occurred infrequently in the dataset (0.03 of values), and importantly similar overall results were obtained regardless if outliers were included or excluded. One-way ANOVAs were used to determine whether CNO altered behavior in *En1^{cre}; Dbh^{Flpo}; RC::FL-hM3Dq* mice. Two-way ANOVAs were used to determine whether the effect of CNO was dependent on mouse genotype. Bonferroni post-hoc tests were conducted when appropriate.

In Vivo Electrophysiology

Animals and Surgery. Multielectrode bundles were surgically implanted in 10 mice with the following genotypes: *Camk2a-cre; RC::L-hM3Dq* (n=4), *Camk2a-cre* (n=3), and *RC::L-hM3Dq* (n=3). Mice, at least 8 weeks of age, were anesthetized with ketamine (100 mg/kg) and xylazine (7 mg/kg) and placed in a stereotax. Four metal anchors and a ground screw were secured in the cranium. A craniotomy was made over the left dorsal hippocampus, and a bundle of 10 wires in medical grade tubing were implanted in the hippocampus using the following stereotaxic coordinates (mm): -2.06 anteroposterior, 2.1 mediolateral, 2.1 dorsoventral from bregma (Paxinos and Franks, 2013). Implanted electrodes were secured to the skull with dental acrylic, and mice were treated with buprenorphine (0.05 mg/kg) to alleviate post-surgical pain.

In Vivo Electrophysiology Recordings. Electrodes were constructed from 44µm polyimide-coated stainless steel wires (Sandvic Materials Technology, Sandviken, Sweden) that connected to a printed circuit board (San Francisco Circuits, San Francisco, CA) and miniature connector (Omnetics Connector Corporation, Minneapolis, MN). Electrode tips were cut to length on the day of surgery. Recordings of neural activity were transmitted via a wireless 32-channel 10x gain headstage (Triangle BioSystems International, Durham, NC) acquired using the Cerebus acquisition system (Blackrock Microsystems, Salt Lake City, UT). Continuous local field potential (LFP) data were band-pass filtered at 0.3–500 Hz and stored at 1,000 Hz. All recordings were referenced to the ground wire connected to a ground screw.

A week after recovery from surgery, recordings were made before, during and after administration of vehicle or CNO. We adopted the dosing regimen used to characterize the original hM3Dq transgene to directly compare our data to prior results (Alexander et al., 2009). Vehicle (1.5% DMSO in saline, i.p.) and the following escalating doses of CNO were administered with 2-3 days between treatments: 0.03, 0.1, 0.3, 0.5, 1, 5 and 10 mg/kg. Electrophysiological recordings were not obtained upon administration of 0.03 or

0.1 mg/kg CNO, but recordings were made upon all other administrations. For all recordings, a baseline period of at least 30 minutes was included before administration of either vehicle or CNO, and recordings were made for 1.5-2 hours following injection. Animals were in a clear plexiglass chamber (20" x 20") during recordings. The experimenter was blind to genotype for all experiments.

Data Analysis for In Vivo Electrophysiology. Analysis of local field potentials (LFPs) were performed using Matlab (version R2014a, MathWorks, Inc., Natick, MA) with Chronux software (http://chronux.org/) (Mitra and Bokil, 2007). LFPs were monitored for the presence of ictal activity following CNO administration. For power spectral analyses of LFPs, spectrograms were first generated to visualize changes in LFP frequency following vehicle or CNO administration. Subsequent power spectral density analyses were used to measure changes in peak gamma (50-80 Hz) power in successive 5-min blocks of LFP data. Peak gamma powers following injection were normalized to pre-injection gamma power, which was calculated by averaging the peak gamma power over the five time bins between 0 and 25 minutes. The 25-30 min time bin was not included in gamma power analysis because mice were handled and injected during this time. Peak gamma powers following vehicle or CNO administration were compared for hM3Dq-expressing and littermate control mice for all treatments using a one- or two-way ANOVA with Bonferroni follow-up tests. Littermate controls heterozygous either for *RC::L-hM3Dq* or *Camk2a-cre* showed no differences in peak gamma power, and thus were combined for analyses.

Body Temperature

Animals and Procedures. Tamoxifen-treated *GFAP-creErt2; RC::L-hM3Dq* double heterozygous mice and littermate controls (N=48, male and female) were tested at 3-5 months of age. Mice (18-29 g) were group housed, with *ad libitum* food and water on a 12:12 light:dark cycle. Mice were restrained to measure baseline body temperature using a rectal probe. Directly after, mice were injected with either vehicle (0.6% DMSO in saline) or CNO (1 or 5 mg/kg, i.p.) and temperature was repeatedly measured every 10 minutes for 90 min post-injection. All mice were tested twice with at least 5 days of recovery between the two tests. A heating pad was made available post-testing to mice exhibiting low-body temperature. Injections were administered at 0.1 mL/10 g using drug prepared fresh daily. The experimenter was blind to drug treatment and genotype for all experiments.

Data Analysis for Body Temperature. Group differences were assessed by one- or two-way ANOVAs followed by Bonferroni multiple comparisons. The results obtained from two repeated vehicle-testing trials were averaged for each subject.

SUPPLEMENTAL REFERENCES

Alexander, G.M., Rogan, S.C., Abbas, A.I., Armbruster, B.N., Pei, Y., Allen, J.A., Nonneman, R.J., Hartmann, J., Moy, S.S., Nicolelis, M.A.*, et al.* (2009). Remote control of neuronal activity in transgenic mice expressing evolved G protein-coupled receptors. Neuron *63*, 27-39.

Mitra, P., and Bokil, H. (2007). Observed Brain Dynamics, 1 edn (USA: Oxford University Press).

Niculescu, D., Hirdes, W., Hornig, S., Pongs, O., and Schwarz, J.R. (2013). Erg potassium currents of neonatal mouse Purkinje cells exhibit fast gating kinetics and are inhibited by mGluR1 activation. J. Neurosci. *33*, 16729-16740.

Nunemaker, C.S., DeFazio, R.A., and Moenter, S.M. (2003). A targeted extracellular approach for recording long-term firing patterns of excitable cells: a practical guide. Biol Proced Online *5*, 53-62.

Paxinos, G., and Franks, K.B.J. (2013). The mouse brain in sterotaxic coordinates (San Diego: Academic Press).

Sciolino, N.R., Smith, J.M., Stranahan, A.M., Freeman, K.G., Edwards, G.L., Weinshenker, D., and Holmes, P.V. (2015). Galanin mediates features of neural and behavioral stress resilience afforded by exercise. Neuropharmacology *89*, 255-264.

Sofroniew, M.V., and Vinters, H.V. (2010). Astrocytes: biology and pathology. Acta Neuropathol. *119*, 7-35.

Sonner, J.M., Cascio, M., Xing, Y., Fanselow, M.S., Kralic, J.E., Morrow, A.L., Korpi, E.R., Hardy, S., Sloat, B., Eger, E.I., 2nd, and Homanics, G.E. (2005). Alpha 1 subunit-containing GABA type A receptors in forebrain contribute to the effect of inhaled anesthetics on conditioned fear. Mol. Pharmacol. *68*, 61-68.

van den Pol, A.N., Ghosh, P.K., Liu, R.J., Li, Y., Aghajanian, G.K., and Gao, X.B. (2002). Hypocretin (orexin) enhances neuron activity and cell synchrony in developing mouse GFP-expressing locus coeruleus. J. Physiol. *541*, 169-185.